High-Order Harmonic Resonances in Traction Power Supplies: A Review Based on Railway Operational Data, Measurements and Experience

Song, Kejian; Wu, Mingli; Yang, Shaobing; Liu, Qiujiang; Agelidis, Vassilios G.; Konstantinou, Georgios

Published in:
IEEE Transactions on Power Electronics

Link to article, DOI:
10.1109/TPEL.2019.2928636

Publication date:
2020

Document Version
Peer reviewed version

This article has been accepted for publication in a future issue of this journal, but has not been fully edited. Content may change prior to final publication. Citation information: DOI 10.1109/TPEL.2019.2928636, IEEE Transactions on Power Electronics

High-Order Harmonic Resonances in Traction Power Supplies: A Review Based on Railway Operational Data, Measurements and Experience

Kejian Song, *Member, IEEE,* Wu Mingli*, *Member, IEEE,* Shaobing Yang, *Member, IEEE,* Qiujiang Liu, Vassilios G. Agelidis, *Fellow, IEEE* and Georgios Konstantinou, *Senior Member, IEEE*

***Abstract*—Harmonic resonances in traction power supply systems (TPSSs) have attracted great attention due to their potentially destructive impact on the safe and stable operation of railways. Based on operation data acquired from Chinese railways, this paper presents a comprehensive review of this issue considering both academic and engineering requirements. Analysing actual incidents, the general patterns and effects of TPSS resonances are derived. The relation between the TPSS and the locomotive is illustrated by circuit models. Relevant methods for modeling locomotives and TPSSs are discussed. Both advanced resonance analysis methods giving general influence factors and a simplified resonance analysis explaining resonance features in a practical manner are discussed. Multiple ground-based and on-board solutions for resonance elimination are presented. At last, pre-identifying resonances in actual systems is investigated for addressing the open topic of resonance prevention.**

***Index Terms*—Electric railway; harmonic resonance; resonance elimination; traction power supply system; traction drive system.**

I. Introduction

RAILWAYS are key infrastructure of national economic importance, forming the backbone of integrated traffic and transport systems for many countries. With the advantages of fast and heavy loading capability, environmentally friendly, electric railways, especially high-speed ones, are becoming popular worldwide. However, their load, electric locomotives, are single-phase, non-linear, rectifying load consuming reactive power, generating harmonics and negative sequence current injected into traction power supply systems (TPSSs) and then into the public grid. Thus, the problem of power quality in the public grid and TPSSs as well as their interaction with the locomotive operation is an old aged but often new issue for both railway and power grid companies all over the world [1]–[8].

This work was supported in part by the Fundamental Research Founds for the Central Universities under Grant 2018JBZ101, and in part by the National Postdoctoral Program for Innovative Talents under Project BX201700026. *(Corresponding author: Wu Mingli.)*

K. Song, W. Mingli*, S. Yang and Q. Liu are with the School of Electrical Engineering, Beijing Jiaotong University, Beijing 100044, China (e-mail: kjsong@bjtu.edu.cn; mlwu@bjtu.edu.cn; shbyang@bjtu.edu.cn; 14117383@bjtu.edu.cn).

V. G. Agelidis is with the Center for Electrical Power and Energy (CEE), Department of Electrical Engineering, Technical University of Denmark, 2800, Kgs. Lyngby, Denmark (email: vasagel@elektro.dtu.dk).

G. Konstantinou is with the School of Electrical Engineering and Telecommunications, The University of New South Wales, Sydney, NSW 2052, Australia (e-mail: g.konstantinou@unsw.edu.au).

Among the reported power quality issues in TPSSs (e.g. power imbalance [9], reactive power [10], low-frequency oscillation and harmonic amplification due to grid-converter instability [11]–[15], harmonic resonance [16], etc.), high-order/frequency harmonic resonances (or simply harmonic resonances) have received great attention by scholars and practitioners [16]–[18]. This problem stems from the use of power electronics in electric locomotive drives. With the development of high power semiconductor devices and associated control techniques, ac-drives have become the most popular choice in traction applications globally [19]–[24]. Ac drive electric locomotives, including electric multiple units (EMUs), use a number of interleaved four-quadrant converters (4QCs) as front-end rectifiers to either draw power from the supply network or inject power back into the supply network during regenerative braking [25]–[27]. Compared with diode and/or thyristor rectifiers of traditional dc electric locomotives [24], the 4QCs ensure unity power factor and a nearly sinusoidal current on the network side. However, the interleaved 4QCs, operating under phase-shifted pulse-width modulation (PS-PWM), still generate relatively high amount of sideband harmonics located around the multiples of the carrier frequency. If some of current harmonics injected into a TPSS coincide with the resonant frequency of this TPSS, a resonance can be excited [28], [29]. When a resonance occurs, amplified resonant voltages and currents appear in the TPSS, resulting in supply voltage distortion, interference with adjacent communication lines, erroneous operation of protective devices, even damaging some high-voltage (HV) devices [30]–[35]. There are two stipulations in the following analysis. Firstly, due to the nature of high-order harmonic resonance, where locomotives are the harmonic source while the TPSS provides the resonance path, the incidents are treated as a power quality issue and not as cases of TPSS instability [36]. Secondly, the high-order harmonic resonance incidents correspond to a parallel resonance which is the main concern in TPSS, while series resonances discussed in some literature, e.g. [37]–[39], are mainly related to background harmonics at lower frequencies seen from an ESS or upper grid.

This article has been accepted for publication in a future issue of this journal, but has not been fully edited. Content may change prior to final publication. Citation information: DOI 10.1109/TPEL.2019.2928636, IEEE Transactions on Power Electronics

A. Previous Studies on TPSS Resonances

An early instance of high-order resonance was encountered in the 1969 test of the first commercial AT (auto-transformer) feeding in the Kagoshima line (Japan) [21]. The cause of the resonance was the large capacitance in the 65-km long supply network, eventually being resolved through the installation of passive filters (PFs) in section posts (SPs). Technical papers reporting TPSS resonances date back to the late 1970s [40], with indications that when two or more electric locomotives haul one train there will be certain risk of resonance which may cause overvoltage and even equipment failure [1]. A digital computer method and an analogue simulation were presented for precalculating the possibility of excessive overvoltage at the early stage of newly designed schemes, with measured resonant voltage from Taiwan railways provided for verification. A damping filter to suppress resonant overvoltages appearing in Zimbabwe national railways was presented in [2]. In the past decades, TPSS resonances in other countries and regions have been reported, e.g. Korea [17], China [41], Czech Republic [42] and Italy [43]. Most studies can be classified into two sets: i) those focusing on network-side modeling to describe the TPSS impedance-frequency characteristics, and ii) those referring to electric locomotive load characteristics to explain how harmonic currents are generated and injected into the overhead supply network.

1) Network-side studies: In early works, wave propagation theory along distributed lines was used to analyse the propagation of harmonic currents generated by electric locomotives. The analysis was based on a "two-transmission line" simplified representation of the 15 kV, 16.7 Hz German TPSS [18]. A method for online identification of resonant frequencies [44] as well as further elimination approaches [45]–[49] were also proposed. However, German railways have special TPSS features such as network structure, voltage and frequency, so resonance related analysis cannot be directly applied to TPSSs in many other countries.

The impedance-frequency characteristics of the Italian 3 kV dc supply network was analysed in [50] and harmonics propagation in the network-locomotive system were investigated through analytical [51] and probabilistic [52] methods. The Korean high-speed railway (HSR) 2×25 kV AT supply network was modeled as an eight-port system, representing the entire system model for harmonic and resonance simulation studies [17]. Similar approaches for the Tehran-Karaj railway in Iran (including both 2×25 kV and 25 kV sections) and the Suvarnabhumi Airport rail link in Thailand (25 kV supply) were presented in [53] and [54], respectively.

2) Locomotive-side studies: The main cause of harmonics in TPSSs is the switching operation of locomotive line-side converters, so explaining harmonic injection from power electronics converters is necessary for TPSS resonance studies. Two different methods for harmonic analysis of the multiple interleaved single-phase, two-level PWM rectifiers [55], [56] were used to explain the generation and frequency characteristics of locomotive line current harmonics. The double Fourier series (DFS), a well-accepted tool for PWM waveform analysis, was adopted for harmonic analysis of two-level [56] and three-level [57], [58] multiple interleaved converters. The impact of dc-link voltage control in the low-order harmonics together with the high-order PWM harmonics was presented in [28], [59] and a probabilistic model of locomotive current harmonics based on operational data was developed in [60].

B. State-of-Art and Operation Experience of Chinese Railways

In China, railway electrification started in the 1960s, somewhat later compared to some European countries and Japan. Since entering the new century, electric railways, especially the high-speed ones, have experienced a very fast growing period. By the end of 2017, Chinese railways covered 127,000 km with 25,000 km of HSRs, accounting for 66.3 % of the total HSR lines globally. The electrification rate is above 65 % with more than 82 % of the transportation task accomplished by electric traction. All electrified lines adopt a standard single-phase, 25 kV[1], 50 Hz ac supply, which is now the most common supply mode worldwide. Since 2007, the HX_D series of ac electric locomotives and the CRH, CR series of EMUs, including a total of more than 20 models, have been successively rolled out. Though all of them used ac drives, i.e., employing 4QCs as line-side converters, the number of interleaved converters and the carrier frequency of each converter are discrepant for different models leading to diverse harmonic spectra.

In a way, due to the long electrified mileage in the common supply mode and the variety of electric locomotives in operation, Chinese railways provide rich operation experience especially incidents related to resonance studies. Since the first high-frequency harmonic resonance occurred back in 2007 in the Beijing-Harbin line, more than 15 other Chinese lines have experienced similar instances. All of the resonances occurred in the 3 kHz frequency span despite being caused by over 10 different models of locomotives and EMUs.

Regarding these resonances, first, a number of field tests have been conducted to identify the features of harmonic resonance, e.g., frequency range, over-voltage/current level [41], [62]–[64]. Then, referring to the measured data, line current harmonics of those locomotive models exciting resonances have been investigated by either DFS analysis [28], [65] or probabilistic modeling [66], [67]. On the other hand, harmonic propagation on the supply network has also been analysed (see [16], [29]–[31], [68]–[73], etc.). Harmonic elimination approaches have been explored from both a TPSS [31], [74] and locomotives perspective [75]–[77]. Recently, [12] and [13] summarised multiple power quality issues (i.e., low-frequency oscillation, harmonic resonance and harmonic instability) in railway electrification systems. Through supply network and electric locomotives modeling in frequency domain and related stability analysis, those issues were defined as a type of network-train instability. In [78], the issue of harmonic

[1]including 2×25 kV mode [61], a special 25 kV supply mode, which provides higher supply capability adopted by HSRs and heavy-haul freight lines.

This article has been accepted for publication in a future issue of this journal, but has not been fully edited. Content may change prior to final publication. Citation information: DOI 10.1109/TPEL.2019.2928636, IEEE Transactions on Power Electronics

resonance of electric railways was independently reviewed from the aspects of identification, mechanism and elimination. The work focused on advanced modeling of the network-train system and verification through simulations and scale-down experiments without strong links to operational data or practical cases of TPSS resonance.

C. Contribution and Organization

Among previous technical papers related to TPSS resonances, there is a lack of comprehensive analysis, linking real incidents with mechanisms that explain resonances and recommend elimination methods. Even if all such aspects can be found in different papers, prevention of resonances remains a key topic open for contributions. This paper contributes to the subject of TPSS resonance, seeing the supply network and locomotives as an interactive system, comprehensively discussing the phenomena, mechanism, elimination and pre-identification based on a large amount of operational data from Chinese railways.

The rest of the paper is organized as follows. Section II discusses two typical TPSS resonance cases providing details on their features and influence, then summarises the TPSS resonance incidents that occurred in Chinese railways over the past decade to conclude general patterns and effects. In Section III, an entire system model is first presented and simplified to illustrate the locomotive-network interaction. Then, modeling methods for both the locomotive side (line current harmonic characteristics) and the TPSS side (impedance-frequency characteristics) are discussed. At last, advanced resonance analysis methods and general influence factors are summarised; considering engineering implementations, a simplified resonance analysis is presented to explain the resonance features in a practical manner. Multiple ground-based and on-board resonance elimination approaches are discussed in Section IV. In Section V, the resonance pre-identification in real systems is investigated for addressing the open topic of resonance prevention. Finally, Section VI summarises this work.

II. Resonance Phenomena on Chinese Railways

A. Case I: 2007, Beijing-Harbin Railway Line

From July to August 2007, reconnection[2] CRH2 EMUs were put into operation in succession on the Beijing-Harbin railway line. During that time, the two sections of the line supplied by the Jixian south electrical substation (ESS), Jixian south ESS to Yanjiao section post (SP) and Jixian south ESS to Hanjialin SP, frequently experienced high-frequency resonances. This led to equipment failure in the network. In Yanjiao SP, catenary network arresters exploded three times and a spark gap broke down once; in Hanjialin SP, dc power charging block and ac power surge protector burnt down; in Jixian south ESS, the reactive power compensation branch breaker tripped frequently leading to branch malfunction.

[2]Generally, a reconnection EMU train has 16 cars consisting of two standard EMUs with 8 cars per each.

Fig. 1. Damage to network HV equipment as a result of TPSS resonances.

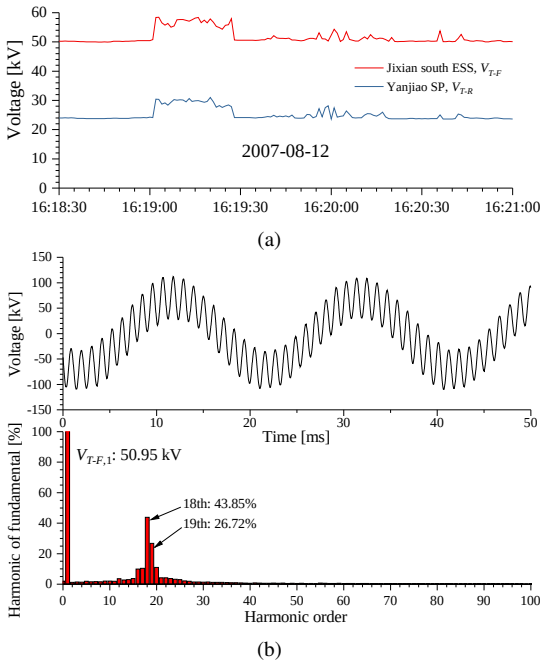

Fig. 2. Measured voltages during resonance, (a) rms of supply voltages at ESS and SP, (b) waveform and spectrum of supply voltage at ESS.

Outside the TPSS, low power appliances (e.g. air conditioners, televisions, low power leakage protectors, etc.) along the two sections were also damaged. Fig. 1 shows the burnt arresters of that incident.

Field tests indicated that CRH2 EMUs were the harmonic source exciting resonance in the 750-1150 Hz (17-23 p.u.) frequency range. Fig. 2(a) shows the rms of supply voltages at Jixian south ESS and Yanjiao SP, which reached 60 kV and 30 kV, respectively[3]. Fig. 2(b) shows the ESS supply voltage waveform and spectrum. Measurements showed a peak value higher than 110 kV with 43.85% of 18th harmonic, 26.72% of 19th harmonic and about 10% of 16th, 17th and 20th harmonics. Meanwhile, the measured rms voltages of indoor power supply in ESS and SPs reached 260 V (nominal 220 V).

B. Case II: 2011, Wuhan-Guangzhou HSR Line

In the afternoon of 23rd January 2011, the section between Guangzhou south ESS and Lishui SP of the Wuhan-

[3]2×25 kV AT supply is adopted in this line. At the ESS, the voltage between catenary wire (T) and feeder wire (F) was measured; and the voltage between T and rails (R) was measured at the SP. During that time, the traction transformer taps of the secondary windings were already turned to 50 kV at the ESS instead of 55 kV for normal operation.

This article has been accepted for publication in a future issue of this journal, but has not been fully edited. Content may change prior to final publication. Citation information: DOI 10.1109/TPEL.2019.2928636, IEEE Transactions on Power Electronics

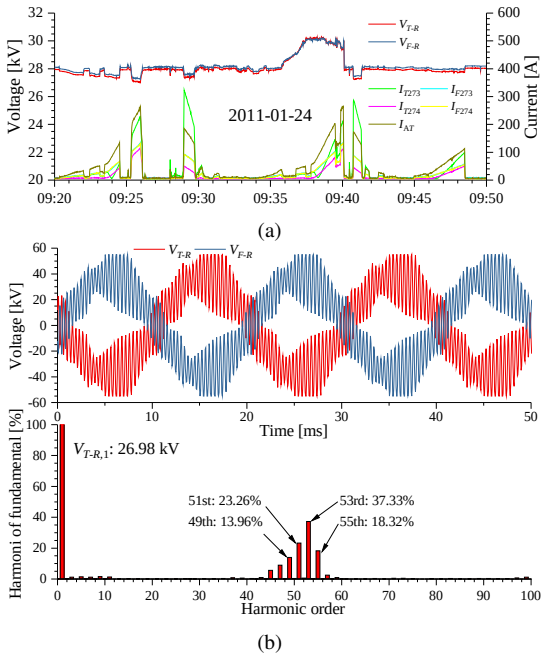

Fig. 3. Measured voltages and currents at SP during resonance, (a) rms of supply voltages and load currents, (b) waveforms and spectrum of supply voltages. (273 and 274 are the labels of down and up links respectively, AT stands for the AT midpoint absorbing current.)

Guangzhou HSR[4] experienced six tripping instances of the breakers due to harmonic resonance, leading to the destruction of four arresters in the catenary network.

Through extensive field tests, it was found that a resonance in the 2250-2750 Hz (45-55 p.u.) frequency range was excited by CRH380A EMUs. Fig. 3(a) shows the measured rms of supply voltages and load currents. Normally, when the load currents increase, the supply voltages will decrease because of the power consumption on the transmission lines. However, from 9:35 a.m. to 9:40 a.m., the CRH380A EMUs that were the main load in this supply section excited the resonance causing supply voltages higher than 30 kV rms. Detailed waveforms and spectrum are given in Fig. 3(b) where the supply voltage, V_{T-R}, contained 37.33% of 53rd harmonic and 23.26% of 51st harmonic. Such high amounts of high frequency harmonics were superimposed onto the fundamental frequency voltage leading to severe overvoltages.

C. Resonance Features and Impacts

Table I summarises 16 resonance incidents[5] that have occurred in Chinese electric railways in the past decade or so. Some key TPSS resonance features include:

i) Frequency: For the 25 kV, 50 Hz supply with 20-40 km long supply sections common in China, the recorded resonant frequencies range from 750 to 3750 Hz. This implies a wide range of potential resonant frequencies. However, for a specific resonant section, the frequency range of harmonic amplification is within 500 Hz, except cases 13 and 14 of Table I.

ii) Overvoltage: A TPSS resonance always results in an overvoltage. Each high-order harmonic voltage in the resonant frequency range can reach several kV, even more than 10 kV for some extreme cases. Such high amount of harmonics can result in peak values higher than 70 kV and rms values higher than 31 kV.

iii) Duration: A resonance event may last between several seconds to minutes, with extreme cases resulting in sustained overvoltage of more than ten minutes. Supply voltage waveforms gradually change to distorted shapes, which have maintained for the duration of the event. In contrast to other general transients, TPSS resonances can be defined as quasi-steady-state phenomena.

iv) Location: Resonances have occurred in sections and stations of HSRs, conventional passenger lines and heavy-haul lines. There is limited correlation between a location and a resonance, but a common feature of the locations will be explained in Section III-D.

v) Vehicle model: Early TPSS resonances in China were mainly excited by CRH2 series[6] EMUs running on HSRs. Later on, the line-side converter controls of those models were improved, significantly decreasing the resonance risk. After 2011, most resonances were excited by HX_D series locomotives running on conventional railways.

On the other hand, the impact of the TPSS resonances can be categorised into two classes:

i) Activation of protection relays: Resonances always trigger overvoltage protections either in the ESSs or on-board the trains, causing breakers to trip. Both ground and on-board breaker tripping actions result in trains stopping, service interruption and delays across the traffic network.

ii) Damages on electrical devices: Both ground and on-board HV devices, especially arresters, may be burnt by resonant overvoltages. In locations where the power grid is too weak to provide independent supply for ESSs and SPs, low power appliances, powered by the traction network through a step-down transformer, may be also damaged. For arresters, the resonant overvoltage with high frequency and high amplitude may increase the leakage current (from several to hundreds mA). When a resonance is sustained for a time interval longer than a few minutes, the arresters may be burnt by overheating of their value plates (usually made by zinc oxide, ZnO).

III. Mechanism of TPSS Resonance

In order to study the resonance mechanism, it is important to identify the interaction between the supply network and the train. Mathematical model for each part of the system need to be formed in the frequency domain. Finally, the TPSS resonance can be defined through impedance-frequency characteristics.

[4]It is now called Beijing-Guangzhou HSR after the Zhengzhou-Wuhan and Beijing-Zhengzhou parts were completed in Sept. and Dec. 2012, respectively.

[5]Other resonance incidents occurred out of China are not included in this table due to lack of detailed data. Interested readers can still find related information from [1], [2], [17], [21], [40], [42], etc.

[6]Technically, the models of CRH2, CHR380A and CRH380AL should be seen as one series.

This article has been accepted for publication in a future issue of this journal, but has not been fully edited. Content may change prior to final publication. Citation information: DOI 10.1109/TPEL.2019.2928636, IEEE Transactions on Power Electronics

TABLE I
RESONANCE CASES IN CHINESE RAILWAYS

No.	Time	Location	Vehicle (f_c [p.u.])*	f_r [p.u.]¶	Main Impact		
					Damaged devices	Breaker tripping	Stopping or delay
1	2007.7-8	Sections of Beijing-Harbin line supplied by Jixian south ESS	CRH2 (25)	15-23	Supply network arresters Appliances in ESS and SP	At ESS	Yes
2	2008.8	Wuqing ESS-Yongle SP of Beijing-Tianjin HSR	CRH2 (25)	25-31	Contact wire arresters (leading power off)	At ESS	Yes
3	2008.12	Sections of Hefei-Nanjing HSR supplied by Longcheng ESS	CRH2 (25)	17	Supply network arrester	None	No
4	2009.4-5	Sections of Hefei-Wuhan HSR supplied by Luan and Chang'anji ESSs	CRH2 (25)	17-21	Unknown	At ESS	Yes
5	2011.1	Zaozhuang-Bengbu over-zone feeding of Beijing-Shanghai HSR	CRH380AL (25)	45-55	Arresters on CRH380BL§	None	No
6	2011.1	Guangzhou south ESS-Lishui SP of Wuhan-Guangzhou HSR	CRH380A (25)	47-55	Supply network arrester	At ESS	Yes
7	2011.11	Shanhaiguan staion	HX_D3B	23-29	RC branches of SS4§	On SS4§	Yes
8	2011.11 -2012.2	Section of Harbin-Dalian Line supplied by Changchun north ESS	HX_D3B	23-29	Arresters on CRH380BL§	None	No
9	2012	Qinjiazhuang ESS-Wuzhai Station of Ningwu-Kelan line	HX_D2 (16)	19-29	Arresters on HX_D2	At ESS	Yes
10	2013.11	Multi-sections of Beijing-Jiulong line between Fuyang and Xiangtang	HX_D1B	53-55	Supply network arresters Arresters on locomotives	HX_D1B	Yes
11	2013.11	Handan SP-locomotive depot of Beijing-Guangzhou line	HX_D2B	41-49	Arresters on locomotives Appliances in ESS and SP	At ESS	Yes
12	2013.11	Wulipu station of Yangpingguan-Ankang line	HX_D21000	41-49	Unknown	None	No
13	2016.3-7	Shanghai EMU depot	CRH380D	63-75	None	On CRH380B§	Yes
14	2016.11	Sections of Beijing-Baotou line supplied by Kongjiazhuang ESS	Unknown†	37-51	Appliances in ESS and SP	None	No
15	2017.4	Sections of Watang-Rizhao line supplied by Liangshan north ESS	Unknown†	19-25	Leading abnormal noise of traction transformer of ESS	None	No
16	2018.5	Section of Qian'an-Caofeidian line supplied by Tanghai ESS	HX_D1 (5)	17-21	Supply network arresters Discharging gap of HX_D2§ RC branches of SS4§	At SP, On HX_D2§	Yes

¶ The frequency of f_r represents the resonant frequency per-unit of 50 Hz.
§ These locomotive models were not the ones initiating the resonances but operating under the resonant supply.
† Multiple models of locomotives were operating under the same supply, but the exact model that initiated the resonance was not identified.
∗ The frequency of f_c represents the carrier frequency of the 4QC modulation per-unit of 50 Hz. The f_c values of HX_D21000, HX_D1B, HX_D2B, HX_D3B and CRH380D are not available.

A. Network-Train Interaction System

The structure of a double-track 2×25 kV AT supply system, which is the most popular choice for HSR and heavy-haul lines worldwide [79]–[81], is presented in Fig. 4(a). A basic TPSS consists of an ESS, a feeding network section, an AT post (ATP) and an SP. The electric locomotives act as nonlinear loads injecting harmonics into the TPSS. In the ESS, a Vx connection transformer is commonly used to draw power from the three-phase public grid (220 kV) and supply two sections. In the feeding network, T, R, F stand for contact wire, rail and feeder wire, respectively. The ATP located at the middle of the section supports the supply voltages. The SP located at the end of a section electrically divides the feeding network.

Treating a locomotive as a constant current source is insufficient for discussing the network-train interaction. As shown in Fig. 4(a), the locomotive is powered by the network through a pantograph, then driven by an ac-dc-ac power conversion system. In practice, the ac-dc stage on the line side is a number of 4QCs interleaved via an on-board step-down transformer with multiple secondary windings. Fig. 4(b) shows a locomotive line-side circuit model with n interleaving 4QCs. Here, v_{abi} $(i = 1, 2, ..., n)$ denotes the 4QC ac-side voltages, while v_p and i_p represent the voltage and current at the pantograph. Z_1 and Z_2 stand for the leakage impedances of the transformer primary and secondary windings, respectively. To simplify the analysis, it is assumed that the transformer turn ratio is 1:1, and all the secondary windings are completely decoupled from each other. Consequently, the circuit can be readily simplified to a Thévenin model coupled with the supply network as shown in Fig. 4(c), where Z_{in} is the equivalent network input impedance seen from the pantograph. Meanwhile, v_L and Z_L stand for the Thévenin equivalent voltage source and

This article has been accepted for publication in a future issue of this journal, but has not been fully edited. Content may change prior to final publication. Citation information: DOI 10.1109/TPEL.2019.2928636, IEEE Transactions on Power Electronics

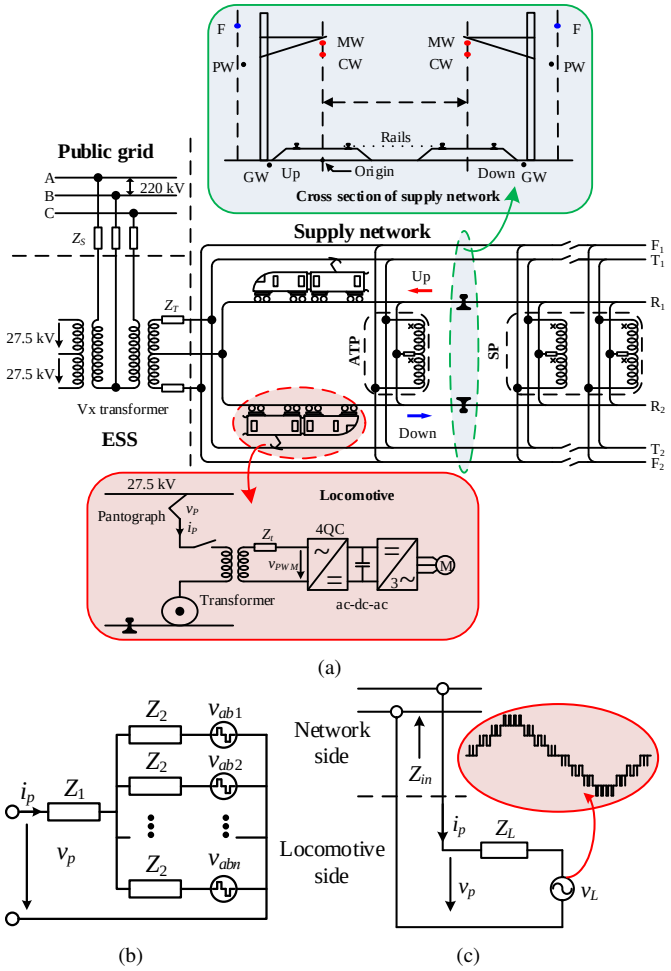

Fig. 4. Network-train interaction, (a) system configuration, (b) equivalent locomotive line-side circuit, (c) Thévenin model of the locomotive coupling with the supply network.

impedance of the locomotive, respectively:

$$v_L = \frac{\sum_{i=1}^{n} v_{abi}}{n}, \tag{1}$$

$$Z_L(j\omega) = Z_1(j\omega) + \frac{Z_2(j\omega)}{n}. \tag{2}$$

The equivalent multi-level PWM voltage v_L is the harmonic source in the system. Neglecting any background harmonics, the k-th harmonic $v_{L,k}$ of v_L generated by the PWM process of 4QCs will give rise to a harmonic voltage $v_{p,k}$ at the pantograph:

$$v_{p,k} = \frac{Z_{in}(jk\omega_1)}{Z_{in}(jk\omega_1) + Z_L(jk\omega_1)} v_{L,k}, \tag{3}$$

where ω_1 stands for the fundamental angular frequency. According to the analysis above, the following can be remarked.

Remark I: Both the equivalent impedances of the TPSS and the locomotive, Z_{in} and Z_L, create a coupling impedance system containing inductive and capacitive elements. The frequencies corresponding to extreme values of this system's impedance-frequency characteristics are the resonant points[7]. The equivalent voltage v_L contains higher-order harmonics which may coincide with the resonant frequency stimulating very high harmonic voltage at the pantograph, $v_{p,k}$, causing a series of detrimental effects, which is collectively referred to as TPSS resonance.

Remark II: The equivalent impedance, Z_{in}, of TPSS refers to the impedance-frequency characteristics of the ESS and the feeding network. The ATs installed in ATP and SP can be omitted from the resonance analysis since their leakage impedances have limited effect on the resonant frequency. Nevertheless, an SP defines the length of a TPSS that affects Z_{in} as well as the resonant frequency. Modeling the complex TPSS in frequency domain is an important aspect of resonance analysis which is significant to get a comprehensive understanding of the resonance mechanism.

B. Modeling of Locomotive Harmonic Characteristics

1) Analytical Method: PS-PWM is generally used for modulating all interleaved 4QCs in a locomotive. DFS can be used to describe one 4QC ac-side PWM voltage waveform in the frequency domain [83], then to express one 4QC ac-side current and entire line current of a train by synthetically considering the circuit parameters and phase shift angles. One can solve the DFS of a PWM waveform by means of 3-dimensional (3-D) [56]–[58] or 2-D [28] graphical method.

Taking a CRH2 series EMU as an example, the DFS expressions of 4QC ac-side voltage and current, v_{ab} and i_{N21}, and the on-board transformer primary current, i_{N1} (mainly consisting of two 4QC ac-side currents, i_{N21} and i_{N22}, for this kind of models) are presented in (4)-(6), respectively. In these equations, V_{dc} and M represent the converter dc-link voltage and the modulation index, J_{2n+1} is the Bessel function of first kind of order $2n+1$, ω_c and ω_o stand for the angular frequencies of carrier and modulation waveforms respectively, θ_c and θ_o are the corresponding initial phase angles. Detailed derivation for (4)-(6) can be found in [28], where the DFS expressions, simulation results and measured data are compared. Through the DFS analysis, one can get:

i) Line-side current harmonics of a locomotive are generated by the modulation process used to shape the 4QC ac-side voltages.

ii) The spectrum of a 4QC line-side current is fairly broad, containing odd sideband harmonics around even multiples of the carrier frequency, i.e., $2m\omega_c + (2n+1)\omega_o$.

iii) For a particular frequency, the modulation index M associated with 4QC output power, is the only factor affecting the harmonic amplitude. It is seen as a coefficient of the independent variable of the Bessel function $J_{2n+1}(2m\pi M)$, which is a bounded function and has a shape of a decaying sinusoidal waveform. M varies within a narrow margin for

[7]Theoretically, there may be more than one resonant frequencies in a TPSS [18], [82]. Fortunately, only the lowest one should be considered for two reasons: this one is easily within the range of the PWM harmonics of lower sideband groups; at higher frequencies the system resistance is high enough to provide a high damping factor [1].

This article has been accepted for publication in a future issue of this journal, but has not been fully edited. Content may change prior to final publication. Citation information: DOI 10.1109/TPEL.2019.2928636, IEEE Transactions on Power Electronics

a PWM rectifier [55], therefore, line current harmonic content is relative stable for different operating conditions of a locomotive.

iv) Neither θ_c or θ_o affect harmonic amplitudes but influence harmonic phases. To properly set θ_c for every 4QCs of a locomotive, i.e., PS-PWM, will effectively eliminate the harmonics of the combined line current. Comparing (5) and (6), harmonics around odd multiples of $2m\omega_c$ are canceled since θ_c of i_{N22} is shifted by $\frac{\pi}{2}$ to that of i_{N21}.

This analytical method is good for understanding the generation mechanism of such harmonics and their influence factors, but is mostly suitable for qualitative analysis. In practice, when quantitatively comparing the analytical harmonic solutions and operational data of locomotive line current, there are certain differences. One of the reasons for these differences is that the derivation process sees the supply voltage as an ideal voltage source, neglecting the interactions between locomotive operation and power transmission on the supply network, e.g. harmonic amplification which will be more apparent when resonances occur. Another reason is that in real systems, there is a number of stochastic factors and parameter nonlinearities which are difficult to be taken into consideration. Besides, the exact technical data for locomotive 4QCs are usually not available leading to imprecise or approximate modeling.

2) Probabilistic Method: An alternative approach providing greater accuracy is to form a probabilistic harmonic model of the locomotive line current based on measurements. Detailed methods can be found in [60], [67] for locomotives with thyristor line-side converters and [66], [84] for locomotives with PWM converters. In brief, the modeling process is as follows:

i) The first step is to describe the ratios of every selected harmonics of locomotive line current including total harmonic distortion (THD). Piecewise curve-fitting can be used on measured data to find proper functions to represent those harmonic ratios varying versus fundamental frequency current or active power.

ii) The second step is to describe the stochastic volatility of the harmonic ratios. The measured data present, in fact, a certain statistical property, i.e., harmonic ratios located around the fitting curves. For each fitting curve, a probability density function, conventionally the well-known Gauss Formula, could be defined to present the distribution property.

iii) The last step is to describe the distribution of harmonic phase angles. Since the angles are affected by the locomotive operation state, i.e., accelerating, constant-speed, regenerative braking and coasting, it is preferable to identify the angles' varying trends for each operation state. Typically, these trends cannot be easily described by simple expressions, so that look-up tables become an option. Fortunately, the angle distribution property along these trends is also subject to the Gauss formula [67].

For a specific locomotive type, through the three-step process above, line current harmonic characteristics will be formed as a probabilistic model which can be used to predict the locomotive line current for simulations at a design stage. Fig. 5 gives a comparison of CRH2 EMU line currents from simulation using probabilistic model and measurements. As the modeling is based on operational data with all the stochastic and nonlinear factors of the real system, the accuracy satisfies the requirements of related quantitative analysis. An obvious drawback of this method is that it considers the line current spectrum as a kind of external feature of the locomotive thus failing to explain how harmonics are generated.

3) Equivalent Locomotive Model to TPSS: When studying issues on the network-train system, e.g. the resonance, a simple locomotive model connected with the TPSS is usually required. Based on DFS solutions and the on-board transformer impedance, a Thévenin model can be formed to represent a locomotive (see Fig. 6(a) as well as Fig. 4(c) with relevant analysis). Alternatively, it can be readily transferred to a Norton model (see Fig. 6(b)). Treating a locomotive as a branch of a TPSS, according to the substitution principle, a simple and useful way is to represent the locomotive by the

$$v_{ab}(t) = V_{dc}M\cos(\omega_o t+\theta_o) + \sum_{m=1}^{\infty}\sum_{n=-\infty}^{\infty}\frac{V_{dc}}{\pi m}J_{2n+1}(2m\pi M)\cos(n\pi)\cos\Big[2m\omega_c t + (2n+1)\omega_o t + 2m\theta_c + (2n+1)\theta_o\Big], \tag{4}$$

$$\begin{aligned} i_{N21}(t) = &\pm\frac{\sqrt{(V_{dcM})^2+2V_{N2}^2}}{\omega_o L}\cos(\omega_o t) \\ &-\sum_{m=1}^{\infty}\sum_{n=-\infty}^{\infty}\frac{V_{dc}}{\pi m[2m\omega_c t + (2n+1)\omega_o]L}J_{2n+1}(2m\pi M)\cos(n\pi)\sin\Big[2m\omega_c t + (2n+1)\omega_o t + 2m\theta_c + (2n+1)\theta_o\Big], \end{aligned} \tag{5}$$

$$\begin{aligned} i_{N1}(t) &= \frac{i_{N21}+i_{N22}}{N_T} \\ &= \frac{1}{N_T}\left\{\begin{array}{l} \pm\dfrac{2\sqrt{(V_{dc}M)^2+2V_{N2}^2}}{\omega_o L}\cos(\omega_o t) \\ -\displaystyle\sum_{m=1}^{\infty}\sum_{n=-\infty}^{\infty}\frac{V_{dc}}{\pi m[4m\omega_c + (2n+1)\omega_o]L}J_{2n+1}(4m\pi M)\cos(n\pi)\sin\left\{\begin{array}{l}4m\omega_c t + (2n+1)\omega_o t \\ +4m\theta_c + (2n+1)\theta_o\end{array}\right\} \end{array}\right\}. \end{aligned} \tag{6}$$

This article has been accepted for publication in a future issue of this journal, but has not been fully edited. Content may change prior to final publication. Citation information: DOI 10.1109/TPEL.2019.2928636, IEEE Transactions on Power Electronics

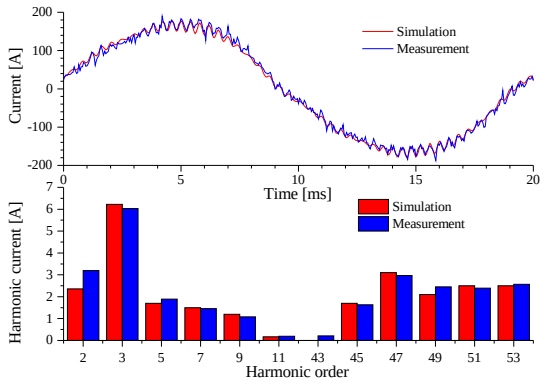

Fig. 5. Comparison of CRH2 EMU line currents from measured data and simulation data by probabilistic model.

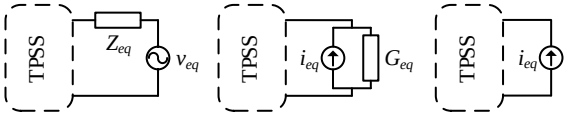

Fig. 6. Equivalent locomotive models to TPSS, (a) Thévenin model, (b) Norton model, (c) current source model.

branch current forming a current source model (see Fig. 6(c)) that could be the line current of analytical solutions, simulation results, probabilistic model based predictions or measured samples.

C. Modeling of TPSS Impedance-Frequency Characteristics

An integrated TPSS impedance consists mainly of three parts: an external power source, an ESS and a section of supply network.

1) External Power Source: When discussing the high-order harmonic resonance in TPSS, the external power source is usually modeled as simple as possible. In practice, limited parameters on grid side are available so that an external power source can be simply modeled as a three-phase Thévenin [85] or Norton [86] equivalent circuit based on the short-circuit capacity and nominal voltage of the primary side of an ESS.

2) Electrical Substation: In the ESS, the main component is the traction transformer which should be expressed by its node admittance matrix. Despite various connections, a traction transformer can be generally described by:

$$\begin{bmatrix} \boldsymbol{I}_P \\ \boldsymbol{I}_S \end{bmatrix} = \begin{bmatrix} \boldsymbol{Y}_{PP} & \boldsymbol{Y}_{PS} \\ \boldsymbol{Y}_{PS}^T & \boldsymbol{Y}_{SS} \end{bmatrix} \begin{bmatrix} \boldsymbol{V}_P \\ \boldsymbol{V}_S \end{bmatrix}, \tag{7}$$

where $\boldsymbol{I}_P$, $\boldsymbol{V}_P$ and $\boldsymbol{I}_S$, $\boldsymbol{V}_S$ are the current and voltage vectors of the transformer primary and secondary sides. Method for forming transformer models with specific connections is referred to [87]. Node admittance matrices of all other elements (e.g. reactive power compensation branches, tuned filters) need to be formulated separately. In the end, an entire ESS model is established by superposing all matrices according to the ESS main connection.

3) Supply Network: Modeling the supply network is a key part of creating an appropriate TPSS impedance-frequency characteristics. Regardless of supply mode (e.g. direct supply (with negative feeder), AT supply, boost transformer (BT) supply [88]), and regardless of the track number (i.e. single or double), the backbone of a supply network are paralleled multiconductor transmission lines (MTL) forming a chain. A chain network model, which is given in Fig. 7(a), was initially introduced for modeling 2×25 kV AT supply network [89], then expanded to a generalised model for describing all types of traction supply networks [90], [91]. This model consists of both series and shunt elements. The shunt elements, i.e., locomotives, ATs or other cross links, split a network into several series segments with different lengths. Each segment is formed by homogeneous series elements, i.e., MTL[8]. The chain network can be described by a node admittance equation of (8), where $\boldsymbol{V}_i$ and $\boldsymbol{I}_i$ $(i = 1, 2, ..., N)$ are the voltage and current vectors at node i. Assuming there are m paralleled conductors in the network, thus $\boldsymbol{Z}_i$ and $\boldsymbol{Y}_i$ $(i = 1, 2, ..., N)$ of (8) are $m \times m$ dimension impedance and admittance matrices. It is clear that the node admittance matrix of the network is a tridiagonal banded matrix which can be easily solved by Schechter LU decomposition. Fig. 7(b) illustrates the method for forming this node admittance: one can firstly formulate node admittance matrix of each series element in a $2m \times 2m$ scale; then superpose all the series element matrices in sequence (two adjacent matrices have a $m \times m$ overlap); finally the network model can be completed by adding the $m \times m$ node admittance matrices of shunt components into the overlaps in sequence.

The MTL of each series segment consisting of m conductors with distributed parameters can be modeled by an equivalent π-type circuit as shown in Fig. 7(c) which is described by:

$$\begin{cases} \boldsymbol{Z}_L = \sinh(\sqrt{\boldsymbol{ZY}}l)(\boldsymbol{ZY})^{-\frac{1}{2}}\boldsymbol{Z} \\ \boldsymbol{Y}_L/2 = \boldsymbol{Y}(\boldsymbol{ZY})^{-\frac{1}{2}}\tanh(\sqrt{\boldsymbol{ZY}}l/2) \end{cases}, \tag{9}$$

where $\boldsymbol{Z}$ and $\boldsymbol{Y}$ are the MTL parameter matrices formed by self- and mutual- impedances and admittances per unit length of the conductors, l stands for segment length. Generally, for a double-track electric railway $m > 10$, which can be reduced by combining the equipotential conductors[9] [92], [93]. To solve (9), both phase-modal transformation [94] and matrix series [95] can be adopted. Modeling of other series and shunt elements of the network, which are relatively easier, can be found in literature, e.g. [91], [96].

For harmonic studies, i.e. resonance, all basic parameters of aforementioned modeling are linked to frequency. In practice, only fundamental parameters of external grid and transformers are usually available, thus they are assumed linear for high-frequency analysis. For MTL, frequency-dependent parameters can be acquired analytically using the conductors' material, shape and spatial position, e.g. through the Carson equation. The skin effect is non-negligible at/close to the resonant

[8]In BT systems the BTs should be seen as series elements as well.

[9]See the cross section of supply network in Fig. 4(a) where conductors with same colors have same potentials.

This article has been accepted for publication in a future issue of this journal, but has not been fully edited. Content may change prior to final publication. Citation information: DOI 10.1109/TPEL.2019.2928636, IEEE Transactions on Power Electronics

$$\begin{bmatrix} \boldsymbol{Y}_1+\boldsymbol{Z}_1^{-1} & -\boldsymbol{Z}_1^{-1} & & & & \\ -\boldsymbol{Z}_1^{-1} & \boldsymbol{Z}_1^{-1}+\boldsymbol{Y}_2+\boldsymbol{Z}_2^{-1} & -\boldsymbol{Z}_2^{-1} & & & \\ & -\boldsymbol{Z}_2^{-1} & \boldsymbol{Z}_2^{-1}+\boldsymbol{Y}_3+\boldsymbol{Z}_3^{-1} & -\boldsymbol{Z}_3^{-1} & & \\ & & \ddots & \ddots & \ddots & \\ & & & -\boldsymbol{Z}_{N-2}^{-1} & \boldsymbol{Z}_{N-2}^{-1}+\boldsymbol{Y}_{N-1}+\boldsymbol{Z}_{N-1}^{-1} & -\boldsymbol{Z}_{N-1}^{-1} \\ & & & & -\boldsymbol{Z}_{N-1}^{-1} & \boldsymbol{Z}_{N-1}^{-1}+\boldsymbol{Y}_N \end{bmatrix} \begin{bmatrix} \boldsymbol{V}_1 \\ \boldsymbol{V}_2 \\ \boldsymbol{V}_3 \\ \vdots \\ \boldsymbol{V}_{N-1} \\ \boldsymbol{V}_N \end{bmatrix} = \begin{bmatrix} \boldsymbol{I}_1 \\ \boldsymbol{I}_2 \\ \boldsymbol{I}_3 \\ \vdots \\ \boldsymbol{I}_{N-1} \\ \boldsymbol{I}_N \end{bmatrix} \tag{8}$$

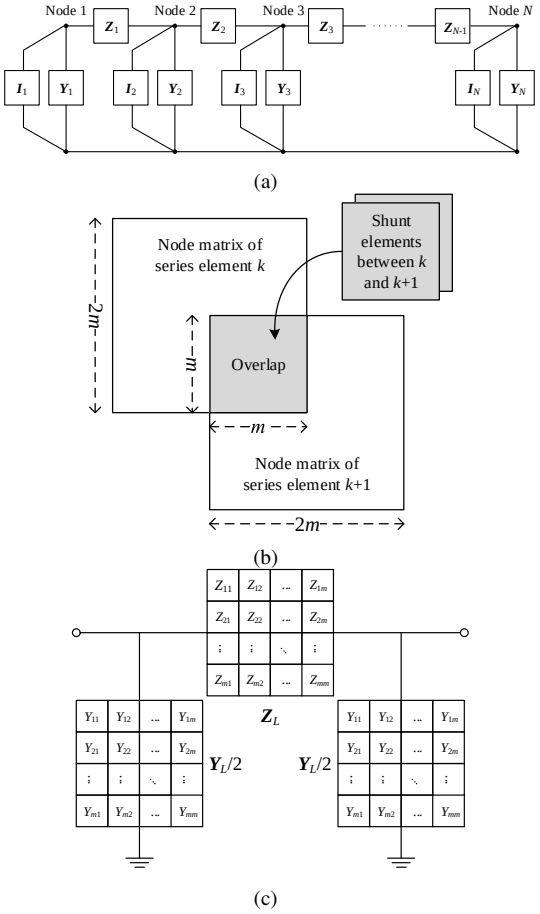

Fig. 7. Modeling of the supply network: (a) chain network model, (b) node admittance forming process, (c) π-type equivalent circuit of series MTL.

frequency where the real and imaginary components of the conductor parameters may have the same order in magnitude [94]. Thus, for an accurate resonance analysis, skin effect formulation should be included into system modeling [97], [98]. In the end, according to specific connections, models of every parts can be linked resulting in a complete TPSS model which is the foundation of harmonic/resonance analysis.

D. Resonance Mechanism Analysis

1) Advanced Analysis Methods: Time-domain simulation (TDS) may be the most efficient approach to test harmonic response in a TPSS and is commonly utilised, e.g. [17], [30], [42], [53], [69], etc.. However, in general simulation environments (Matlab/Simulink, PSCAD/EMTDC, etc.) the accuracy is limited for the following reasons: the distributed supply network can just be represented by lumped RLC cells

TABLE II
ADVANCED RESONANCE ANALYSIS METHODS

Methods	Advantages	Disadvantages
TDS	Higher efficiency	Lower accuracy
FS	Great accuracy Parallel & series resonance Explicit physical meaning	Scan nodes one by one No sensitivity information
RMA	Sensitivity information Quantizes component impact	No straight link between mode number & node location Complex process

with arbitrary defined small lengths; implementing frequency-dependent RLC parameters is not possible; the skin effect or other nonlinearities are also hard to be included.

More accurate analysis is usually carried out by means of frequency scan (FS) [82] and resonance mode analysis/assessment (RMA) [96]. The FS is based on the calculation acting on system node admittance, $\boldsymbol{Y}_s$, which has a inverse, $\boldsymbol{Y}_s^{-1} = \boldsymbol{Z}_s$, with impedance nature. Its element z_{s-ij} is defined as driving impedance and scanned in frequency range of interest, yielding the information that how much voltage at node i will be excited by 1 p.u. current injected into node j; the maxima and minima of the resulted impedance-frequency curve indicate parallel and series resonances, respectively.

The RMA is based on the eigen-analysis, which transfers the system into modal domain, i.e., $\boldsymbol{Y}_s \rightarrow \boldsymbol{Y}_{sm}$. The parallel resonances can be identified through modal analysis which results in sensitivity information of the components of a complex system. Details of the RMA are provided in [99], [100] and [96] for its application for TPSS resonances. The main advantages and disadvantages of FS and RMA as well as TDS are summarised in Table II[10].

A number of factors impacting the resonance in terms of frequency and magnitude are available regardless of the analysis methods leveraged. However, some, especially the quantitative ones, are quite dependent to specific cases studied with detailed parameters. From literature ([17], [53], [69], [82], [96], etc.), there are some general findings for the primary parallel resonance concerned: i) the MTL of supply network and traction transformer in ESS dominate the TPSS resonance, other elements (e.g. external grid) have less prominent effect; ii) longer distance of the supply network corresponds to lower resonant frequencies; iii) resonant harmonics tend to be amplified more at the far-end of a supply section; iv) the resonance magnitude will decrease when increasing inductive

[10]Other methods, e.g. S-domain analysis from control and stability angle, are not discussed here since their application to TPSS resonance needs further study.

This article has been accepted for publication in a future issue of this journal, but has not been fully edited. Content may change prior to final publication. Citation information: DOI 10.1109/TPEL.2019.2928636, IEEE Transactions on Power Electronics

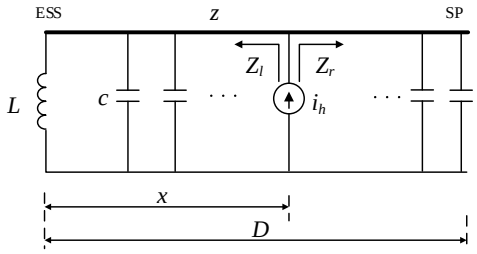

Fig. 8. Simplified circuit model of traction power supply systems.

parameters; an opposite effect will be obtained by increasing capacitive parameters; v) the resonant frequency can be simply seen independent of the train location[11], however, the resonant amplification is more apparent when the train is located further away from the ESS.

2) Simplified Analysis: When addressing real resonant incidents, it is preferable to use simpler modeling and analysis methods. Therefore, a simplified resonance mechanism analysis is adopted here. A TPSS can be simplified as an equivalent model (Fig. 8), where L is the equivalent inductor of the ESS (mainly the transformer leakage impedance and the equivalent impedance of external power source), z and c stand for the series impedance and parallel capacitance of the equivalent single-phase circuit per unit length, i_h represents the locomotive (as current harmonic source), D and x are the distances from the ESS to the SP and the locomotive, respectively.

The equivalent impedance seen from the harmonic source to the ESS (left) is [1]:

$$Z_l = Z_c \frac{j\omega L \cosh(\gamma x) + Z_c \sinh(\gamma x)}{j\omega L \sinh(\gamma x) + Z_c \cosh(\gamma x)}, \tag{10}$$

where $Z_c = \sqrt{z/j\omega c}$ and $\gamma = \sqrt{j\omega c z}$ are the characteristic impedance and propagation constant of the equivalent single-phase circuit, respectively. The equivalent impedance seen from the harmonic source to the SP (right) is:

$$Z_r = \frac{Z_c}{\tanh\big[\gamma(D-x)\big]}. \tag{11}$$

The integrated impedance of the TPSS seen from the harmonic source is:

$$Z = Z_l // Z_r = \frac{Z_l Z_r}{Z_l + Z_r} \tag{12}$$

$$= Z_c \cosh\big[\gamma(D-x)\big] \frac{j\omega L \cosh(\gamma x) + Z_c \sinh(\gamma x)}{j\omega L \sinh(\gamma D) + Z_c \cosh(\gamma D)}. \tag{13}$$

According to (13), it is easy to find $Z = \infty$ at the resonant frequency, implying:

$$j\omega L = \frac{-Z_c}{\tanh(\gamma D)}. \tag{14}$$

[11]Heuristic finding from [96] indicates that resonant frequency moves a bit when train location changes. In fact, the impact of train location and number is still an aspect needs further study especially for the cases of hub stations where many trains operate under a same supply.

Since $\gamma D \ll 1$, $\tanh(\gamma D) \approx \gamma D$, eq. (14) can be rewritten as:

$$j\omega L \approx \frac{-Z_c}{\gamma D} = \frac{-1}{j\omega c D} = \frac{-1}{j\omega C}, \tag{15}$$

where $C = cD$ is the total parallel capacitance of the whole supply network. Therefore, from (15), an approximate resonant frequency equation is acquired:

$$f \approx \frac{1}{2\pi\sqrt{LC}}. \tag{16}$$

According to the analysis above, the following conclusions about TPSS resonance can be reached:

i) Inherently, the TPSS resonance can be seen as a parallel resonance between the distributed capacitance of the supply network and the equivalent inductance of the ESS, always stimulating overvoltages in the TPSS.

ii) The TPSS resonant frequency depends on its own distributed electrical parameters of the supply network, the impedance frequency characteristics of the transformer and external power source of the ESS. The location of the locomotive within a section does not affect the resonant frequency.

iii) Under the same conditions of external power source, transformer and conductors (supply network), the longer a supply section length is, the larger its parallel capacitance (C) leading to lower resonant frequencies. There is an approximately inversely proportional relationship between the resonant frequency of a supply section to the square root of its length.

These useful conclusions from the simplified analysis readily explain the resonance phenomena summarised in Table I of Section III: a parallel resonance always excites overvoltage damaging electrical devices or triggering the protective relay; for a specific TPSS section (see each case of Table I), the frequency range of harmonic amplification is fixed, however different sections have different resonant frequencies because of divergent ESSs and supply networks. Although the incidents took place in different zones, they share a common condition, long equivalent parallel supply networks leading to lower resonant frequencies which are prone to be excited by PWM harmonics of electric locomotives or EMUs.

IV. Resonance Elimination

Since the resonance is related to both the TPSS and electric locomotive, one can eliminate it through ground-based and on-board approaches.

A. Ground-based Harmonic Suppression

1) Installing Passive Filters in ESSs/SPs: Passive filters (PFs), consisting of RLC elements without complex control, are structurally simple, easy to design and reliable. Typical PF topologies of power industry are analysed in [101] and their features are summarised in Table III.

In railway supplies, single-tuned filters (STFs) are usually installed in ESSs to filter out the low-order harmonics; the first-order high-pass filter (1-HPF), i.e. series RC, can be an option addressing higher-order harmonic issues (e.g. applied in

This article has been accepted for publication in a future issue of this journal, but has not been fully edited. Content may change prior to final publication. Citation information: DOI 10.1109/TPEL.2019.2928636, IEEE Transactions on Power Electronics

TABLE III
ADVANTAGES AND DISADVANTAGES OF TYPICAL PASSIVE FILTERS

Topologies	Advantages	Disadvantages
STF	Strong attenuation Low cost	Frequency specific Introduce resonances
1-HPF	Simple structure with HP nature	Require large capacitor Large fundamental loss
2-HPF	Best HP performance	Large fundamental loss (but less than 1-HPF)
3-HPF	Good HP performance low fundamental loss	Introduce resonances
CTF	Better HP performance low fundamental loss	Sensitive to parameter variation

South Korea [102]); second-order HPFs (2-HPFs), also named as second order damping filters (SODFs), are an effective solution to TPSS resonances (applied in Japan [21], Zimbabwe [2] and China [74]); third-order HPFs (3rd HPFs) are not a common choice in this application; C-type filters (CTFs) with their promising features, have certain potential in TPSS for harmonic problems [31].

Fig. 9(a) presents the main circuits of SODFs with their connection to 25 kV and 2×25 kV TPSSs. Fig. 9(b) shows a set of SODF equipment which is installed in the Changchun north sub-feeder switching post (SFSP) to solve the resonances (case 8 of Table I). As a result, the supply voltage there has been filtered to a nearly sinusoidal waveform after the SODF operation, as shown in Fig. 9(c). Up to now, 12 sets of SODFs have been installed and commissioned in ESSs and SPs in Chinese railways. Instances of harmonic resonance in these sections have been successfully eliminated.

Note that all PFs, regardless of topology, do not only filter out harmonics but move resonant frequencies. Despite their high cost and additional land requirements, installing them in ESSs or SPs is a simple, reliable and validated approach for addressing harmonic resonance issues.

2) Installing Active Power Filters in ESSs/SPs: Active power filters (APFs) have been widely used in the electric utility industry for power quality regulation owing to their distinct advantages of small size, controllable output (both frequency and amplitude) and compatible compensation (reactive power, voltage drop and imbalance) compared to traditional PFs [103]–[106]. Nevertheless, APFs are still not a common choice in TPSS applications. According to the technical literature (e.g. [107], [108]), a step-down transformer is usually designed to match the voltage level between the IGBTs and the traction supply network. As reported in [109], [110], a set of straight hanging APF based on cascaded H-bridge (CHB) is designed and installed in an ESS of Beijing-Shanghai HSR line. This is, up to now, the only APF in use in the Chinese railways.

Unfortunately, APFs usually compensate harmonics lower than the 11st. In a word, for the purpose of TPSS resonance elimination, current APF techniques are hard to simultaneously satisfy the requirements of high capacity (several MVA), high voltage (line to ground 27.5 kV) and real-time high-frequency precise control for high-order harmonic compensation (microsecond precision). However, with the development of wide band-gap semiconductor devices (SiC), using APFs to solve power quality issues of TPSSs is still a promising application.

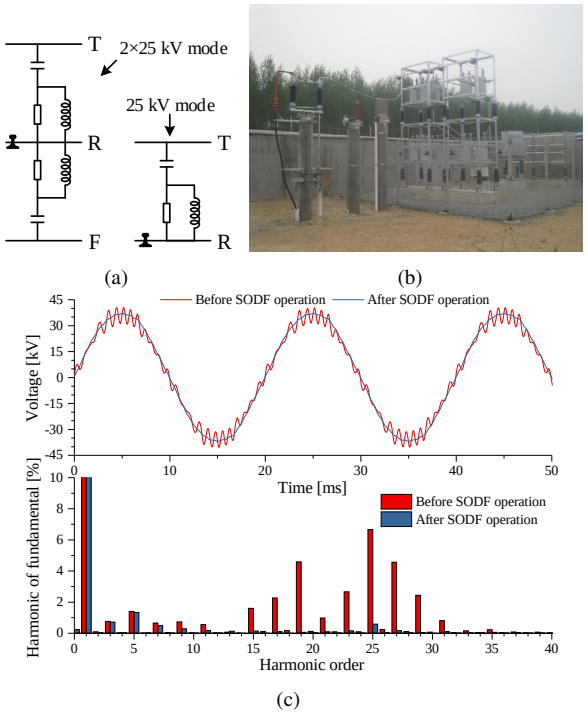

Fig. 9. Application of second-order damping filters for resonance elimination in Chinese railways, (a) main circuits, (b) photo of the actual installation, (c) elimination performance.

3) Other Provisional Measures on the Ground: Other approaches include: i) *switching the external power source of the ESS*, ii) *changing the supply network operation mode* (e.g. changing over-zone supply), etc. These approaches, that efficiently change the TPSS impedance-frequency characteristics (resonant frequency) without the time or cost of construction of the two previous methods, can be provisional measures for resonance suppression.

B. On-Board Harmonic Suppression

1) Conventional PS-PWM: Generally, a locomotive or an EMU has a number of interleaved 4QCs operating under PS-PWM for getting a higher equivalent switching frequency and lower harmonic content. This is the most conventional on-board harmonic suppression approach [56], [58]. In practice, in June 2009, the PS-PWM scheme and controller parameters of the 4QCs of CRH2-200 EMUs were upgraded to improve the line current harmonic characteristics. A set of comparative spectra of CRH2-200 EMU line current measured before and after the upgrade is given in Fig. 10. Since then, few resonances stimulated by CRH2 series EMUs (See Table I).

2) Improved PWM methods: From the PWM perspective, a properly designed PWM scheme that does not generate harmonic components within the resonant frequency range is a straightforward solution. At this point, selective harmonic elimination PWM (SHE-PWM) with its distinct advantage of tight spectrum control [111] can be chosen as an alternative

This article has been accepted for publication in a future issue of this journal, but has not been fully edited. Content may change prior to final publication. Citation information: DOI 10.1109/TPEL.2019.2928636, IEEE Transactions on Power Electronics

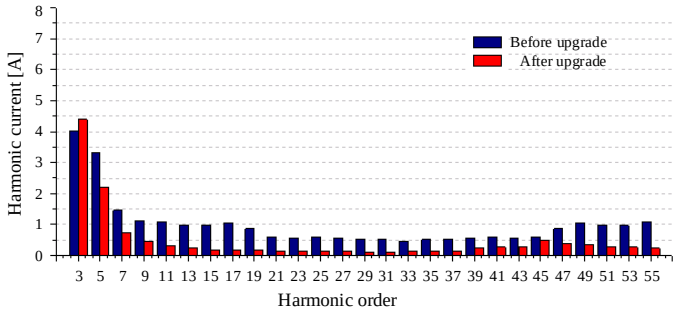

Fig. 10. CRH2-200 EMU line current harmonic spectra before and after the PS-PWM scheme upgrade.

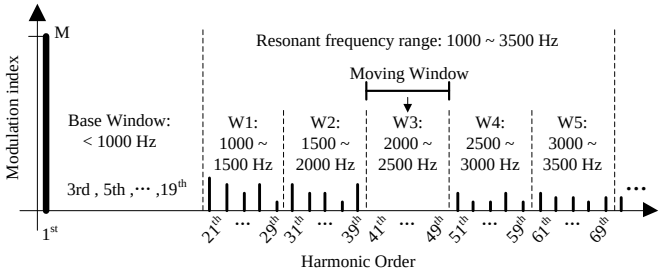

Fig. 11. Concept of windowed SHE-PWM utilising W3, eliminating resonant harmonics between 2000 and 2500 Hz.

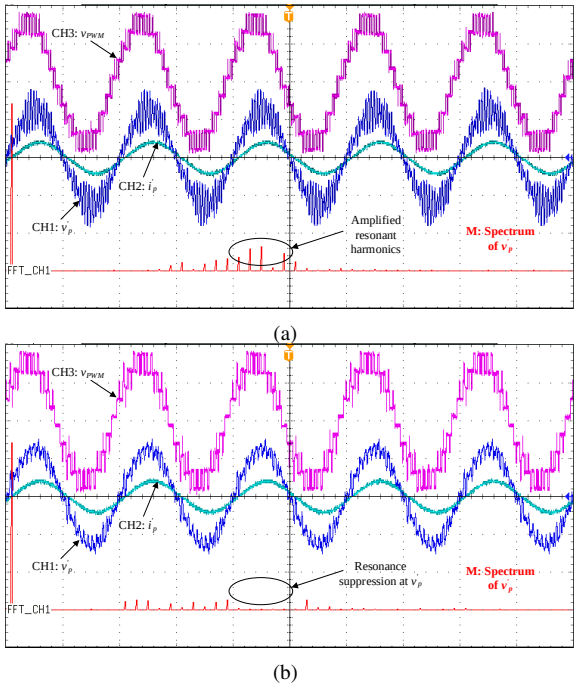

Fig. 12. Experimental result on the resonant circuit: (a) PS-PWM with 250 Hz carrier frequency, (b) windowed SHE-PWM with W3, M = 0.71. CH1: v'_p, 100 V/div, CH2: i'_p, 20 A/div, CH3: v_{PWM}, 100 V/div, M: FFT for CH3, 20 V/div-y, 500 Hz/div-x.

to traditional PS-PWM. In [112], SHE-PWM was initially introduced for two interleaved EMU 4QCs, but the resonance issue was not considered in that work. A SHE-PWM, named resonant harmonic elimination PWM (RHEPWM), was proposed in [75] for resonant harmonic elimination. Nevertheless, the RHEPWM provides a fixed SHE-PWM pattern for a specific resonant frequency, it fails to tackle the resonant frequency variation when the train travels across different supply sections (Section III-D).

The windowed SHE-PWM (WSHE-PWM) scheme for interleaved 4QCs of [76] provides two distinct windows of eliminated harmonics: a base window (BW) fixed in low frequency range plus a moving window (MW) within the potential resonant frequency range (see Fig. 11). In the BW, the fundamental component is controlled to specific modulation index, M, and all the odd harmonics are eliminated. The MW addresses the resonance for a particular TPSS section and can move accordingly. The frequency range of potential resonances is split into several sub-regions, W1-W5; each of them is with a frequency width equal to the MW. When the resonant frequency is in a sub-region, all harmonics within the window are eliminated. Figs. 12(a) and (b) present a set of experimental performance of PS-PWM and WSHE-PWM with same equivalent switching frequency and equivalent resonant circuit applied. The differences of the equivalent pantograph voltage, v'_p, on both waveform shapes and spectra show the resonant harmonic elimination effect of the WSHE-PWM. Interested readers are refered to [76] for details of WSHE-PWM and more papers, e.g. [113], [114], for methods about solving SHE-PWM problem of multiple interleaved and multi-level cases.

However, it should be noted that implementing a low frequency SHE-PWM scheme in a closed-loop system is not a trivial task. As a result, there are few successful cases of SHE-PWM used in traction 4QCs applications, despite its inherent suitability for the purpose of resonance elimination.

3) On-board filters: Some earlier models of electric locomotives, such as the German Class 120 locomotive, the Chinese SS4 locomotive and the CRH1 EMU [18], [115], were equipped with RLC based PFs connecting to either the primary or secondary windings of the on-board transformer. Thus, in most situations, harmonics can be suppressed from the generation-end. In contrast, an on-board PF offers a low damping path absorbing resonant harmonic currents from the overhead line in case of a section already being in resonance stimulated by other locomotives. In general, the PF capacity, which is designed for a single locomotive, is inadequate for a whole section. Such PFs, especially their resistors, can be easily burnt during extreme resonances. Considering the reliability, volume and cost, a number of new locomotive models have abandoned this filter design approach.

An alternative is an on-board APF which provides controllable frequency-domain characteristics compared to on-board PF and has lower capacity and voltage requirements compared to ground APF. German and Japanese researchers proposed similar solutions [48], [116]; adding an auxiliary winding to the on-board transformer and connecting an APF to the additional winding. This APF is used to compensate all the harmonic currents from the 4QCs connected on secondary windings. Mainly restricted by the switching frequency of the IGBTs fitted, on-board APFs cannot cover all potential

This article has been accepted for publication in a future issue of this journal, but has not been fully edited. Content may change prior to final publication. Citation information: DOI 10.1109/TPEL.2019.2928636, IEEE Transactions on Power Electronics

TABLE IV
TPSS RESONANCE ELIMINATION APPROACHES

Approaches	Advantages	Disadvantages
Ground based		
PFs	Simple and reliable for resonance elimination	Large land requirement High cost Large power consumption
APF	Smaller than PFs Controllable output	Limited to low-order harmonics Less reliable than PFs
Other provisional measures	Fast implementation Low cost	Limited elimination effect
On board		
PS-PWM	Easy to implement	Generate fixed side-band harmonics
SHE-PWM	Controllable spectra	Difficult to implement
PFs & APFs	Smaller sizes, lower power and voltages than ground based counterparts	Need space in carriages Train reliability

resonant frequency ranges. A hybrid solution with active and passive filters for locomotives, consisting of an APF, an RC branch and an SODF, can also be used [117]. Full-scale experimental results show that in the hybrid system, the higher-order harmonics are filtered through the SODF, the APF plays the role of lower-order harmonic compensator, and the RC branch absorbs sideband harmonics generated by the APF itself. The main advantages and disadvantages of the TPSS resonance elimination approaches discussed above are summarised in Table IV.

V. IDENTIFICATION OF RESONANCES IN REAL SYSTEMS

Generally, one treats TPSS resonances as sporadic issues taking elimination measures after a resonance incident occurs. Practically, it is hard to prevent TPSS resonances. On the one hand, there is a large number of electric locomotive models with diverse line-side current harmonic features. Moreover, details of modulation schemes and control strategies of the locomotive line-side converters (i.e., the 4QCs), are confidential to the manufacturers, but important for resonance elimination. Although harmonic features of locomotives could be found from their type-test reports, TPSS resonant frequencies are difficult to accurately calculate, predict or evaluate through a model-based analytical way.

A. Assessing TPSS resonant frequencies

The resonant frequencies of a TPSS depend on the impedance-frequency characteristics of both the supply network and the ESS (Section III-C and Section III-D). However, the extremely high diversity of sections in the railway network, in terms of lengths, structure, construction (i.e. bridges, tunnels, etc.) together with non-linearities, especially the skin effect in the conductors, creates a large number of permutations and introduces complexities in mathematical modeling as well as implementation in a time-domain simulation environment such as MATLAB/Simulink or PSCAD.

Furthermore, the harmonic impedance of the external power supply, which supplies and is also part of the ESS impedance, is typically not carefully considered when modeling the TPSS in the high-frequency harmonic range. In fact, network configuration and customer loads connected to the external power supply will affect the harmonic impedance and the resonant frequencies of a given TPSS. Reliable parameter estimation of impedances from model-based calculation or assessment is typically limited to 20 p.u. in frequency and does not cover the whole range of possible resonant frequencies [118], [119].

In short, lack of comprehensive data, the almost infinite number of permutations and non-ideal behaviour of the actual system pose severe difficulties in accurately calculating TPSS resonant frequencies.

B. Resonant frequency measurement

An alternative to model-based calculations for identifying the resonant frequencies of a TPSS is based on harmonic injection and measurement through a power electronics based harmonic generator (HG) [120]–[122].

The concept of TPSS resonant frequency measurement based on the HG is shown in Fig. 13(a). The HG is connected between the catenary and the rail, similar to a locomotive. A harmonic current i_g is then injected into the TPSS resulting in a harmonic voltage v_g as a response. Neglecting background harmonics, the equivalent input impedance of the TPSS at the test location can be calculated as follows:

$$Z_{TPSS}(f_g) = |Z_{TPSS}|\angle\theta_{TPSS} = \frac{v_g(f_g)}{i_g(f_g)}, \qquad (17)$$

where f_g is the objective harmonic frequency of generated current i_g. Through a frequency sweep across the range of interest, the TPSS impedance-frequency characteristics can be acquired. The peak value of (17) corresponds to the resonant frequency of the TPSS under measurement.

How the HG generates a current with arbitrary spectrum becomes a power electronics issue. As shown in Fig. 13(b), the HG is based on a standard CHB converter connecting to the TPSS through a reactor, L, and a step-down transformer. In simple terms, this is a very feasible plan to control harmonic up to thousands Hz[12] at the voltage level of 27.5 kV. Through dedicated control and modulation process, the CHB ac-side composite voltage v_{CHB} can be fully controlled, injecting current i_g with harmonic controllable in both frequency and amplitude. In practice, inter-harmonics can be generated to enhance measurement precision and minimise error from background noise. Interested readers are referred to [121], [122] for details of the measuring method and the HG.

Utilising the proposed measuring method and HG, a first test was carried out in May 2018 on a newly designed Chinese HSR line. Configuration of the field test is given in Appendix A. Fig. 13(c) provides a set of impedance-frequency characteristics of a TPSS section measured at ESS and SP, respectively, illustrating the following:

[12]In practical implementation, 5000 Hz is set for the developed HG as the upper limit to cover the potential resonant frequency range.

This article has been accepted for publication in a future issue of this journal, but has not been fully edited. Content may change prior to final publication. Citation information: DOI 10.1109/TPEL.2019.2928636, IEEE Transactions on Power Electronics

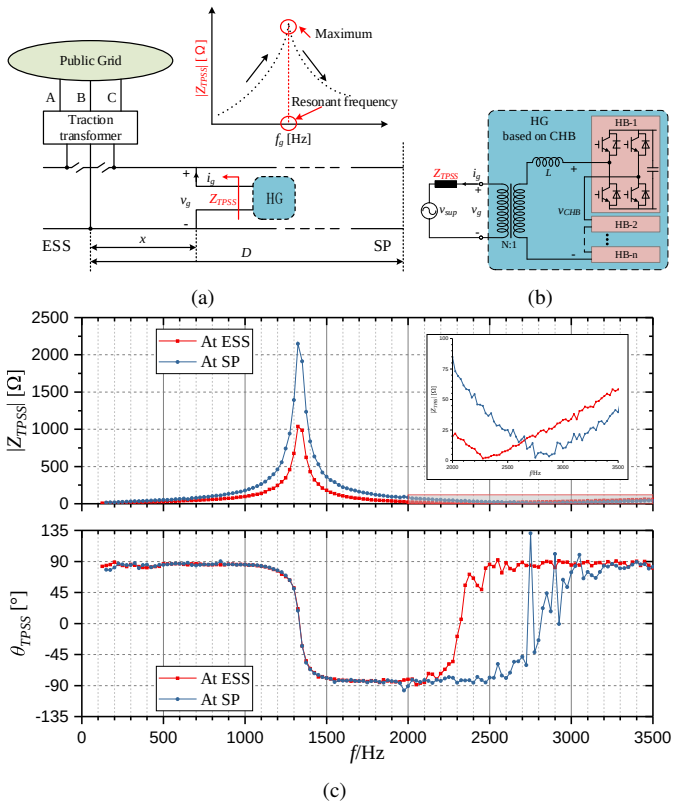

Fig. 13. TPSS resonant frequency identification based on harmonic injection measuring method: (a) concept of the method, (b) circuit model of HG, (c) TPSS impedance-frequency characteristics measured in an actual system.

Primary resonance: A parallel resonant point is identified at 1325 Hz where $|Z_{TPSS}|$ shows a maximum. As expected, this frequency is independent of the test location. However, the maximum $|Z_{TPSS}|$ at this frequency seen from tail end (SP) is about twice of that seen from the head end (ESS). The phase response, θ_{TPSS}, gives additional information: the system is almost purely inductive at low frequencies (<1000 Hz); the system turns to almost purely capacitive (>1500 Hz), after crossing through the resonant point where the system behavior is resistive; all these features can be readily explained by a LC parallel circuit like Fig. 8.

Series resonance: Although not the main concern, series resonant points are also identified. Zooming in $|Z_{TPSS}|$ at high frequencies (>2000 Hz), two minima at approximately 2325 Hz and 2825 Hz appear for ESS and SP test results respectively; θ_{TPSS} shows that at these frequencies the system is resistive, and crossing them turns the system from capacitive to inductive. It confirms that the further a test point to ESS, the higher series resonance is [69].

Testing error: At high frequencies, the measured θ_{TPSS} deviate from their expected trajectories for reasons such as the decreasing phase-angle precision of the current sensor and the higher electromagnetic noise introduced from the environment.

Knowledge of the TPSS impedance-frequency characteristics is a key requirement in providing methods to prevent resonances. These methods will be beneficial to the commissioning of newly designed railway lines and locomotives.

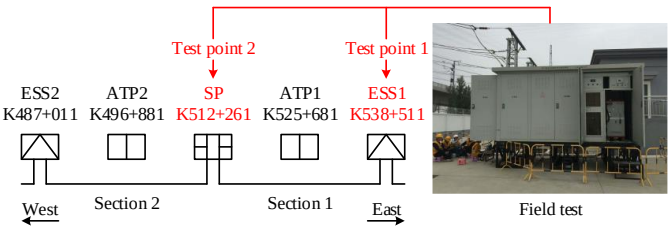

Fig. 14. Field test configuration for measuring TPSS impedance frequency characteristics.

VI. Discussion and Summary

This paper addressed the issue of TPSS resonance, discussing phenomena, mechanism as well as elimination and pre-identification. The provided analysis is based on a large amount of data, extensive measurements and operation experience from Chinese railways over the past decade. Considering both academic and engineering requirements, the work is expected to provide a comprehensive overview of this issue to both researchers and practitioners in the field.

In summary, the high-order harmonic resonance is a typical power quality issue linked to both the TPSSs (impedance frequency characteristics) and the electric locomotives (line current harmonic characteristics). The two parts constitute an interaction system; the former as the dominant resonant circuit that carries the energy flow and the later playing the role of harmonic source that generates high-frequency harmonics injected into the system. Occurrence of harmonic resonance depends on the coincidence of the two in frequency.

Although resonances in TPSSs have occurred for decades, they still represent an unsolved issue in railway supply. The basis to figure out this issue is to break the resonant conditions at either the TPSS or the locomotive side. Practical experience shows that simpler engineering approaches should be considered before resolving to advanced elimination methods. For future work, if reliable information on the locomotive current harmonics and TPSS resonant frequencies can be acquired, prevention at the design stage is a more efficient approach to elimination after an event.

Appendix A
Field Test Configuration

Fig. 14 demonstrates the test sections and points of the line attached with a photo from the field testing. By switching the breakers in ESSs, SP and ATPs, a 51.5 km long line (from ESS2 at K487+011 to ESS1 at K538+511 including over-zone supply) was set to 11 operation modes. As a result, the TPSS impedance frequency characteristics under all these modes were obtained. The results in Fig. 13(c) are of section 1 (from ESS1 at K538+511 to SP at K512+261) operating under all parallel 2×25 kV AT supply mode (This is the normal operation mode for Chinese HSRs where the supply network of up and down tracks are connected in parallel at ESS, ATP and SP to provide higher current-carrying capability and more redundancy.).

REFERENCES

[1] R. E. Morrison and M. J. Barlow, "Continuous overvoltages on ac traction systems," *IEEE Power Engineering Review*, vol. PER-3, no. 5, pp. 37–38, May 1983.

[2] R. E. Morrison and J. C. W. Corcoran, "Specification of an overvoltage damping filter for the national railways of zimbabwe," *IEE Proceedings B - Electric Power Applications*, vol. 136, no. 6, pp. 249–256, Nov. 1989.

[3] R. J. Hill, "Electric railway traction. part 3. traction power supplies," *Power Engineering Journal*, vol. 8, no. 6, pp. 275–286, Dec. 1994.

[4] J. Arrillaga, *Power System Quality Assessment*. Chichester: John Wiley & Sons, 2001.

[5] E. Mollerstedt and B. Bernhardsson, "Out of control because of harmonics-an analysis of the harmonic response of an inverter locomotive," *IEEE Control Systems*, vol. 20, no. 4, pp. 70–81, 2000.

[6] A. Steimel, *Electric traction - motive power and energy supply*. Munich: Oldenbourg Industrieverlag GmbH, 2008.

[7] L. Sainz, L. Monjo, S. Riera, and J. Pedra, "Study of the steinmetz circuit influence on ac traction system resonance," *IEEE Trans. Power Del.*, vol. 27, no. 4, pp. 2295–2303, Oct. 2012.

[8] A. Župan, A. T. Teklić, and B. Filipović-Grčić, "Modeling of 25 kv electric railway system for power quality studies," in *Eurocon 2013*, Jul. 2013, pp. 844–849.

[9] Z. Shu, S. Xie, and Q. Li, "Single-phase back-to-back converter for active power balancing, reactive power compensation, and harmonic filtering in traction power system," *IEEE Trans. Power Electron.*, vol. 26, no. 2, pp. 334–343, Feb. 2011.

[10] S. Gazafrudi, A. Tabakhpour Langerudy, E. Fuchs, and K. Al-Haddad, "Power quality issues in railway electrification: A comprehensive perspective," *IEEE Trans. Ind. Electron.*, vol. 62, no. 5, pp. 3081–3090, May 2015.

[11] H. Wang, W. Mingli, and J. Sun, "Analysis of low-frequency oscillation in electric railways based on small-signal modeling of vehicle-grid system indqframe," *IEEE Trans. Power Electron.*, vol. 30, no. 9, pp. 5318–5330, Sep. 2015.

[12] H. Hu, H. Tao, F. Blaabjerg, X. Wang, Z. He, and S. Gao, "Train–network interactions and stability evaluation in high-speed railways–part i: Phenomena and modeling," *IEEE Trans. Power Electron.*, vol. 33, no. 6, pp. 4627–4642, Jun. 2018.

[13] H. Hu, H. Tao, X. Wang, F. Blaabjerg, Z. He, and S. Gao, "Train–network interactions and stability evaluation in high-speed railways—part ii: Influential factors and verifications," *IEEE Trans. Power Electron.*, vol. 33, no. 6, pp. 4643–4659, Jun. 2018.

[14] X. Zhang, J. W. Spencer, and J. M. Guerrero, "Small-signal modeling of digitally controlled grid-connected inverters with lcl filters," *IEEE Trans. Ind. Electron.*, vol. 60, no. 9, pp. 3752–3765, Sep. 2013.

[15] L. Harnefors, X. Wang, A. G. Yepes, and F. Blaabjerg, "Passivity-based stability assessment of grid-connected vscs—an overview," *IEEE Journal of Emerging and Selected Topics in Power Electronics*, vol. 4, no. 1, pp. 116–125, Mar. 2016.

[16] Z. He, H. Hu, Y. Zhang, and S. Gao, "Harmonic resonance assessment to traction power-supply system considering train model in china high-speed railway," *IEEE Trans. Power Del.*, vol. 29, no. 4, pp. 1735–1743, Aug. 2014.

[17] H. Lee, C. Lee, G. Jang, and S. hyuk Kwon, "Harmonic analysis of the korean high-speed railway using the eight-port representation model," *IEEE Trans. Power Del.*, vol. 21, no. 2, pp. 979–986, Apr. 2006.

[18] J. Holtz and H. J. Kelin, "The propagation of harmonic currents generated by inverter-fed locomotives in the distributed overhead supply system," *IEEE Trans. Power Electron.*, vol. 4, no. 2, pp. 168–174, Apr. 1989.

[19] R. Wagner, "Ac drive technology for locomotives," in *Proceedings., Technical Papers Presented at the IEEE/ASME Joint Railroad Conference*, Apr. 1989, pp. 1–5.

[20] K. Sato, M. Yoshizawa, and T. Fukushima, "Traction systems using power electronics for shinkansen high-speed electric multiple units," in *Proc. Int. Power Electron. Conf.*, Jun. 2010, pp. 2859–2866.

[21] T. Uzuka, "Faster than a speeding bullet: An overview of japanese high-speed rail technology and electrification," *IEEE Electrification Magazine*, vol. 1, no. 1, pp. 11–20, Sep. 2013.

[22] X. Huang, L. Zhang, M. He, X. You, and Q. Zheng, "Power electronics used in chinese electric locomotives," in *Proc. IEEE Int. Power Electron. and Motion Control Conf.*, May 2009, pp. 1196–1200.

[23] H.-S. Song, R. Keil, P. Mutschler, J. van der Weem, and K. Nam, "Advanced control scheme for a single-phase pwm rectifier in traction applications," in *Proc. Annu. Meeting, Ind. Appl. Conf.*, vol. 3, Oct. 2003, pp. 1558–1565 vol.3.

[24] G. G. Balazs, M. Horvath, I. Schmidt, and P. Kiss, "Examination of new current control methods for modern pwm controlled ac electric locomotives," in *Proc. IET Int. Conf. Power Electron., Machines and Drives*, Mar. 2012, pp. 1–5.

[25] W. Song, J. Ma, L. Zhou, and X. Feng, "Deadbeat predictive power control of single-phase three-level neutral-point-clamped converters using space-vector modulation for electric railway traction," *IEEE Trans. Power Electron.*, vol. PP, no. 99, pp. 1–1, 2015.

[26] L. He, J. Xiong, H. Ouyang, P. Zhang, and K. Zhang, "High-performance indirect current control scheme for railway traction four-quadrant converters," *IEEE Trans. Ind. Electron.*, vol. 61, no. 12, pp. 6645–6654, Dec. 2014.

[27] A. Steimel, "Electric railway traction in europe," *IEEE Ind. Appl. Mag.*, vol. 2, no. 6, pp. 6–17, Nov. 1996.

[28] S. Kejian, W. Mingli, V. Agelidis, and W. Hui, "Line current harmonics of three-level neutral-point-clamped electric multiple unit rectifiers: analysis, simulation and testing," *IET Power Electron.*, vol. 7, no. 7, pp. 1850–1858, Jul. 2014.

[29] X. Chu, F. Lin, and Z. Yang, "The analysis of time-varying resonances in the power supply line of high speed trains," in *Proc. Int. Power Electron. Conf.*, May 2014, pp. 1322–1327.

[30] Y. Xiong, Y. Zhang, and D. Tong, "Analysis on harmonic current of electrified railway traction network based on multi-port reduced-order model," in *Proc. China Int. Conf. Electricity Distribution*, Sep. 2012, pp. 1–6.

[31] H. Hu, Z. He, and S. Gao, "Passive filter design for china high-speed railway with considering harmonic resonance and characteristic harmonics," *IEEE Trans. Power Del.*, vol. 30, no. 1, pp. 505–514, Feb. 2015.

[32] BS EN 50163: 2004, "Railway applications - supply voltages of traction systems," *BSI Standards Publication*, Nov. 2004.

[33] IEC 60850: 2014, "Railway applications - supply voltages of traction systems," *International Electrotechnical Commission*, Nov. 2014.

[34] IEC 610000-3-6: 2008, "Electromagnetic compatibility (emc) - part 3-6: Limits - assessment of emission limits for the connection of distorting installations to mv, hv and ehv power systems," *International Electrotechnical Commission*, Feb. 2008.

[35] GB/T 14549-1993, "Quality of electric energy supply - harmonics in public supply network," *China National Standard*, 1993 (In Chinese).

[36] BS EN 50388: 2012, "Railway applications - power supply and rolling stock - technical criteria for the coordination between power supply (substation) and rolling stock to achieve interoperability," *BSI Standards Publication*, Aug. 2012.

[37] X. Sun, J. Zeng, and Z. Chen, "Site selection strategy of single-frequency tuned r-apf for background harmonic voltage damping in power systems," *IEEE Transactions on Power Electronics*, vol. 28, no. 1, pp. 135–143, Jan. 2013.

[38] L. Sainz, M. Caro, and E. Caro, "Analytical study of the series resonance in power systems with the steinmetz circuit," *IEEE Trans. Power Del.*, vol. 24, no. 4, pp. 2090–2098, Oct. 2009.

[39] L. Sainz, J. Pedra, and M. Caro, "Background voltage distortion influence on power electric systems in the presence of the steinmetz circuit," *Electric Power Systems Research*, vol. 79, no. 1, pp. 161–169, 2009.

[40] K. Halva and P. Havel, "Resonances in traction supply circuit 25kv 50hz," *Proceedings of railway research intitute*, Prague, 1976, (In Czech).

[41] "Research on the abnormal supply voltage of jixiannan traction substation of beijing-harbin railway line: measurement, analysis and elimination method," *Report by Beijing Railway Bureau, Beijing Jiaotong University, China Railway Electrification Survey Design & Research Institute CO., LTD and China Academy of Railway Sciences*, 2007, (In Chinese).

[42] V. Kolar, J. Palecek, S. Kocman, T. T. Vo, P. Orsag, V. Styskala, and R. Hrbac, "Interference between electric traction supply network and distribution power network - resonance phenomenon," in *Proceedings of 14th International Conference on Harmonics and Quality of Power - ICHQP 2010*, Sep. 2010, pp. 1–4.

[43] M. Brenna, A. Capasso, M. C. Falvo, F. Foiadelli, R. Lamedica, and D. Zaninelli, "Investigation of resonance phenomena in high speed railway supply systems: Theoretical and experimental analysis," *Electric Power Systems Research*, vol. 81, no. 10, pp. 1915–1923, Oct. 2011.

[44] J. Holtz and J. O. Krah, "On-line identification of the resonance conditions in the overhead supply line of electric railways," *Archiv Für Elektrotechnik*, vol. 74, no. 1, pp. 99–106, 1990.

[45] J. Holtz and J. O. Krah, "Adaptive optimal pulse-width modulation for the line-side converter of electric locomotives," *IEEE Trans. Power Electron.*, vol. 7, no. 1, pp. 205–211, Jan. 1992.

[46] J. Holtz and J. O. Krah, "Suppression of time-varying resonances in the power supply line of ac locomotives by inverter control," *IEEE Transactions on Industrial Electronics*, vol. 39, no. 3, pp. 223–229, Jun. 1992.

[47] J. Holtz and L. Springob, "Reduced harmonics pwm controlled line-side converter for electric drives," *IEEE Transactions on Industry Applications*, vol. 29, no. 4, pp. 814–819, Jul. 1993.

[48] J. O. Krah and J. Holtz, "Total compensation of line-side switching harmonics in converter-fed ac locomotives," *IEEE Trans. Ind. Appl.*, vol. 31, no. 6, pp. 1264–1273, Nov. 1995.

[49] M. Ogasa, J. O. Krah, and J. Holtz, "Harmonic compensator for 50-hz fed ac railway vehicles," in *Proceedings of Power Conversion Conference - PCC '97*, vol. 1, Aug. 1997, pp. 57–62 vol.1.

[50] P. Ferravi, A. Maviscotti, and P. Pozzobon, "Reference curves of the pantograph impedance in dc railway systems," in *2000 IEEE International Symposium on Circuits and Systems. Emerging Technologies for the 21st Century. Proceedings (IEEE Cat No.00CH36353)*, vol. 1, May 2000, pp. 555–558 vol.1.

[51] P. Pinato and D. Zaninelli, "Harmonic disturbances in electric traction system overhead lines," in *Harmonics and Quality of Power, 2002. 10th International Conference on*, vol. 2, Oct. 2002, pp. 748–753 vol.2.

[52] F. Foiadelli, G. Lazaroiu, and D. Zaninelli, "Probabilistic method for harmonic analysis in railway system," in *Power Engineering Society General Meeting, 2005. IEEE*, Jun. 2005, pp. 2397–2401 Vol. 3.

[53] F. Mehdavizadeh, S. Farshad, S. V. Raygani, and M. R. Shahroudi, "Resonance verification of tehran-karaj electrical railway," in *2010 First Power Quality Conferance*, Sep. 2010, pp. 1–6.

[54] B. Lutrakulwattana, M. Konghirun, and A. Sangswang, "Harmonic resonance assessment of 1×25kv, 50hz traction power supply system for suvarnabhumi airport rail link," in *2015 18th International Conference on Electrical Machines and Systems (ICEMS)*, Oct. 2015, pp. 752–755.

[55] J. Taufiq and J. Shen, "Frequency domain modelling of traction pwm converters," in *Power Electronics and Applications, 1993., Fifth European Conference on*, Sep. 1993, pp. 63–67 vol.7.

[56] J. Shen, J. Taufiq, and A. Mansell, "Analytical solution to harmonic characteristics of traction pwm converters," *IEE Proceedings - Electric Power Applications*, vol. 144, no. 2, pp. 158–168, Mar. 1997.

[57] J. Shen and N. Butterworth, "Analysis and design of a three-level pwm converter system for railway-traction applications," *IEE Proceedings - Electric Power Applications*, vol. 144, no. 5, pp. 357–371, Sep. 1997.

[58] G. W. Chang, H.-W. Lin, and S.-K. Chen, "Modeling characteristics of harmonic currents generated by high-speed railway traction drive converters," *IEEE Trans. Power Del.*, vol. 19, no. 2, pp. 766–773, Apr. 2004.

[59] J. Huang, Y. Lu, B. Zhang, N. Wang, and W. Song, "Harmonic current elimination for single-phase rectifiers based on pr controller with notch filter," in *Electrical Machines and Systems (ICEMS), 2012 15th International Conference on*, Oct. 2012, pp. 1–5.

[60] R. E. Morrison and A. D. Clark, "Probabilistic representation of harmonic currents in ac traction systems," *IEE Proceedings B - Electric Power Applications*, vol. 131, no. 5, pp. 181–189, Sep. 1984.

[61] C. Courtois, "Why the 2*25 kv alternative? (autotransformer traction supply)," in *IEE Colloquium on 50kV Autotransformer Traction Supply Systems - the French Experience*, Nov. 1993, pp. 1/1–1/4.

[62] "Technique research report of the high-order harmonic impact of ac drive electric locomotives," *Report by Beijing Jiaotong University*, 2010, (In Chinese).

[63] "Measurement and analysis report of abnormal supply voltage of the debug workshop of crrc changchun railway vehicles co., ltd," *Report by Beijing Jiaotong University*, 2012, (In Chinese).

[64] "Research report of voltage oscillation of high-speed railways," *Report by CRRC Qingdao Sifang CO., LTD*, 2012, (In Chinese).

[65] H. Cui, X. Feng, and W. Song, "Modeling of high-order harmonic load for high speed train," *Electric Power Automation Equipment*, vol. 33, no. 7, pp. 92–99, 2013, (In Chinese).

[66] Y. Shaobing, H. Mei, and W. Mingli, "High speed emu modeling based on the measured data," in *2009 International Conference on Sustainable Power Generation and Supply*, Apr. 2009, pp. 1–4.

[67] Y. Shaobing and W. Mingli, "Dynamic load modelling of electric locomotive for power quality assessment of utilities," in *Railway Traction Systems (RTS 2010), IET Conference on*, Apr. 2010, pp. 1–5.

[68] H. Cui, X. Feng, L. Xuan, Q. Wang, and S. J. University, "Research on harmonic resonance characteristic of high-speed railway traction net considering coupling of trains and traction nets," *Transactions of China Electrotechnical Society*, vol. 28, no. 9, pp. 54–64, 2013, (In Chinese).

[69] L. Guo, Q. Li, and Y. Xu, "Study on harmonic resonance of traction line in electrified high-speed traction system," in *2009 International Conference on Sustainable Power Generation and Supply*, Apr. 2009, pp. 1–4.

[70] H. Hu, Z. He, X. Li, K. Wang, and S. Gao, "Power-Quality Impact Assessment for High-Speed Railway Associated With High-Speed Trains Using Train Timetable—Part I: Methodology and Modeling," in *IEEE Trans. Power Del.*,vol. 31, no. 2, pp. 693–703, Apr. 2016.

[71] H. Hu, P. Pan, Y. Song, and Z. He, "A Novel Controlled Frequency Band Impedance Measurement Approach for Single-phase Railway Traction Power System," in *IEEE Trans. Ind. Electron.*, pp. 1–1, 2019 (early access article).

[72] H. Tao, H. Hu, X. Wang, F. Blaabjerg, and Z. He, "Impedance-based harmonic instability assessment in a multiple electric trains and traction network interaction system," *IEEE Trans. Ind. Appl.*, vol. 54, no. 5, pp. 5083–5096, Sep. 2018.

[73] Z. Li, H. Hu, Y. Zhou, and Z. He, "A rapid modal analysis method for harmonic resonance using modified power iteration," *IEEE Trans. Power Del.*, vol. 33, no. 3, pp. 1495–1497, Jun. 2018.

[74] W. Mingli, Z. Huang, S. Yang, Z. Chu, and M. Liu, "Suppression device for higher-order harmonic resonance and transient over-voltage in traction network," in *CHN Patent: ZL 2007 1 0120620.9*, Sep. 2007.

[75] H. Cui, W. Song, H. Fang, X. Ge, and X. Feng, "Resonant harmonic elimination pulse width modulation-based high-frequency resonance suppression of high-speed railways," *IET Power Electron.*, vol. 8, no. 5, pp. 735–742, 2015.

[76] K. Song, G. Konstantinou, W. Mingli, P. Acuna, R. P. Aguilera, and V. G. Agelidis, "Windowed she-pwm of interleaved four-quadrant converters for resonance suppression in traction power supply systems," *IEEE Trans. Power Electron.*, vol. 32, no. 10, pp. 7870–7881, Oct. 2017.

[77] Z. Runze, L. Fei, Y. Zhongping, C. Hu, and L. Yuping, "Active resonance suppression strategy for grid-train coupling resonance based on she-pwm," *Transactions of China Electrotechnical Society*, vol. 33, no. zk1, pp. 129–138, 2018, (In Chinese).

[78] H. Hu, Y. Shao, L. Tang, J. Ma, Z. He, and S. Gao, "Overview of harmonic and resonance in railway electrification systems," *IEEE Trans. Ind. Appl.*, vol. 54, no. 5, pp. 5227–5245, Sep. 2018.

[79] J. P. Menuet, "The autotransformer and other equipment (for railway power supply)," in *IEE Colloquium on 50kV Autotransformer Traction Supply Systems - the French Experience*, Nov. 1993, pp. 3/1–3/4.

[80] R. Cella, , A. Mariscotti, A. Montepagano, P. Pozzobon, M. Ruscelli, and M. Vanti, "Measurement of at electric railway system currents at power-supply frequency and validation of a multiconductor transmission-line model," *IEEE Trans. Power Del.*, vol. 21, no. 3, pp. 1721–1726, Jul. 2006.

[81] M. Brenna and F. Foiadelli, "Sensitivity analysis of the constructive parameters for the 2 × 25-kv high-speed railway lines planning," *IEEE Trans. Power Del.*, vol. 25, no. 3, pp. 1923–1931, Jul. 2010.

[82] A. Dolara, M. Gualdoni, and S. Leva, "Impact of high-voltage primary supply lines in the 2 × 25 kv - 50 hz railway system on the equivalent impedance at pantograph terminals," *IEEE Trans. Power Del.*, vol. 27, no. 1, pp. 164–175, Jan. 2012.

[83] D. G. Holmes and T. A. Lipo, *Pulse Width Modulation for Power Converters : Principles and Practice*. IEEE, 2003.

[84] S. Yang and M. Wu, "Study on harmonic distribution characteristics and probability model of high speed emu based on measured data," *Journal of the China Railway Society*, vol. 32, no. 3, pp. 33–38, 2010, (In Chinese).

[85] T.-H. Chen, "Criteria to estimate the voltage unbalances due to high-speed railway demands," *IEEE Trans. Power Syst.*, vol. 9, no. 3, pp. 1672–1678, Aug. 1994.

[86] H. Hu, Z. He, K. Wang, X. Ma, and S. Gao, "Power-quality impact assessment for high-speed railway associated with high-speed trains using train timetable—part ii: Verifications, estimations and applications," *IEEE Trans. Power Del.*, vol. 31, no. 4, pp. 1482–1492, Aug. 2016.

[87] T. H. Chen and H. . Kuo, "Network modelling of traction substation transformers for studying unbalance effects," *IEE Proceedings - Gener-*

ation, Transmission and Distribution, vol. 142, no. 2, pp. 103–108, Mar. 1995.

[88] J. D. Glover, A. Kusko, and S. M. Peeran, "Train voltage analysis for ac railroad electrification," *IEEE Trans. Ind. Appl.*, vol. IA-20, no. 4, pp. 925–934, Jul. 1984.

[89] H. Fujie, "Program attc-p for analyzing the power characteristics of at feeder circuit," *Power Quality Reports*, vol. 24, no. 2, pp. 87–88, 1983.

[90] M. Wu, "Research on electical parameters and mathematic models of traction power supply system," Ph.D. dissertation, Beijing Jiaotong University (BJTU), 2006, (In Chinese).

[91] W. Mingli, C. Roberts, and S. Hillmansen, "Modelling of ac feeding systems of electric railways based on a uniform multi-conductor chain circuit topology," in *Proc. IET Conf. Railway Traction Systems*, Apr. 2010, pp. 1–5.

[92] W. Mingli and F. Yu, "Numerical calculations of internal impedance of solid and tubular cylindrical conductors under large parameters," *IEE Proceedings - Generation, Transmission and Distribution*, vol. 151, no. 1, pp. 67–72, Jan. 2004.

[93] W. Mingli, "Physical interpretation of impedance formulas for conductors enclosed in a cylindrical tunnel," *IEEE Trans. Power Del.*, vol. 26, no. 3, pp. 1354–1360, Jul. 2011.

[94] J. Arrillaga, T. J. Densem, and J. Harker, "Zero sequence harmonic current generation in transmission lines connected to large convertor plant," *IEEE Transactions on Power Apparatus and Systems*, vol. PAS-102, no. 7, pp. 2357–2363, July 1983.

[95] M. Wu and Q. Li, "A study of harmonic model and its algorithms for transmission lines," *Journal of the China Railway Society*, vol. 17, no. a01, pp. 105–112, 1995, (In Chinese).

[96] Z. He, H. Hu, Y. Zhang, and S. Gao, "Harmonic resonance assessment to traction power-supply system considering train model in china high-speed railway," *IEEE Trans. Power Del.*, vol. 29, no. 4, pp. 1735–1743, Aug. 2014.

[97] S. D. A., E. Kennelly, F. H. Achard, and A. S. Dana, "Experimental researches on the skin effect in steel rails," *Journal of the Franklin Institute*, vol. 182, no. 2, pp. 135–189, 1916.

[98] R. A. Chipman, *Theory and problems of transmission lines*. Schaums Outline Series McGraw-Hill, 1968.

[99] W. Xu, Z. Huang, Y. Cui, and H. Wang, "Harmonic resonance mode analysis," *IEEE Trans. Power Del.*, vol. 20, no. 2, pp. 1182–1190, Apr. 2005.

[100] Y. Cui and W. Xu, "Harmonic resonance mode analysis using real symmetrical nodal matrices," *IEEE Trans. Power Del.*, vol. 22, no. 3, pp. 1989–1990, Jul. 2007.

[101] A. B. Nassif, W. Xu, and W. Freitas, "An investigation on the selection of filter topologies for passive filter applications," *IEEE Trans. Power Del.*, vol. 24, no. 3, pp. 1710–1718, Jul. 2009.

[102] H. Lee, G. Kim, S. Oh, and C. Lee, "Optimal design for power quality of electric railway," in *Proc. Int. Joint Conf. SICE-ICASE*, Oct. 2006, pp. 3864–3869.

[103] H. Akagi, "Trends in active power line conditioners," *IEEE Trans. Power Electron.*, vol. 9, no. 3, pp. 263–268, May 1994.

[104] H. Akagi, "New trends in active filters for power conditioning," *IEEE Trans. Ind. Appl.*, vol. 32, no. 6, pp. 1312–1322, Nov. 1996.

[105] B. Singh, K. Al-Haddad, and A. Chandra, "A review of active filters for power quality improvement," *IEEE Trans. Ind. Electron.*, vol. 46, no. 5, pp. 960–971, Oct. 1999.

[106] M. El-Habrouk, M. K. Darwish, and P. Mehta, "Active power filters: A review," *IEE Proceedings - Electric Power Applications*, vol. 147, no. 5, pp. 403–413, Sep. 2000.

[107] Z. Sun, X. Jiang, D. Zhu, and G. Zhang, "A novel active power quality compensator topology for electrified railway," *IEEE Trans. Power Electron.*, vol. 19, no. 4, pp. 1036–1042, Jul. 2004.

[108] A. Bueno, J. M. Aller, J. A. Restrepo, R. Harley, and T. G. Habetler, "Harmonic and unbalance compensation based on direct power control for electric railway systems," *IEEE Trans. Power Electron.*, vol. 28, no. 12, pp. 5823–5831, Dec. 2013.

[109] L. Wu and W. Mingli, "Single-phase cascaded h-bridge multi-level active power filter based on direct current control in ac electric railway application," *IET Power Electronics*, vol. 10, no. 6, pp. 637–645, 2017.

[110] L. Wu, "Power quality compensation technology in electric railways based on 27.5 kv straight hanging cascaded apf," Ph.D. dissertation, Beijing Jiaotong University (BJTU), 2017, (In Chinese).

[111] H. S. Patel and R. G. Hoft, "Generalized techniques of harmonic elimination and voltage control in thyristor inverters: Part i–harmonic elimination," *IEEE Trans. Ind. Appl.*, vol. IA-9, no. 3, pp. 310–317, May 1973.

[112] G. Konstantinou, V. G. Agelidis, and J. Pou, "Interleaved selective harmonic elimination pwm for single-phase rectifiers in traction applications," in *Proc. IEEE Annu. Conf. Ind. Electron. Soc.*, Nov. 2013, pp. 930–935.

[113] G. Konstantinou, V. G. Agelidis, and J. Pou, "Theoretical considerations for single-phase interleaved converters operated with she-pwm," *IEEE Power Electron. Lett.*, vol. 29, no. 10, pp. 5124–5128, Oct. 2014.

[114] M. S. A. Dahidah, G. Konstantinou, and V. G. Agelidis, "A review of multilevel selective harmonic elimination pwm: Formulations, solving algorithms, implementation and applications," *IEEE Trans. Power Electron.*, vol. 30, no. 8, pp. 4091–4106, Aug. 2015.

[115] Z. Yang, X. Huang, S. Wu, and H. Peng, "Traction technology for chinese railways," in *The 2010 International Power Electronics Conference - ECCE ASIA -*, Jun. 2010, pp. 2842–2848.

[116] T. Maeda, T. Watanabe, A. Mechi, T. Shiota, and K. Iida, "A hybrid single-phase power active filter for high order harmonics compensation in converter-fed high speed trains," in *Proc. Conf. Power Conversion*, vol. 2, Aug. 1997, pp. 711–717 vol.2.

[117] Z. Zhang, Z. Zhang, and C. Huang, "Harmonic restraining devices on locomotives," *Electric Drive for Locomotives*, no. 5, pp. 17–21, Sep. 2016, (In Chinese).

[118] A. Robert, T. Deflandre, E. Gunther, R. Bergeron, A. Emanuel, A. Ferrante, G. S. Finlay, R. Gretsch, A. Guarini, and J. L. G. Iglesias, "Guide for assessing the network harmonic impedance," in *Electricity Distribution*, 1997, pp. 3/1–310 vol.2.

[119] A. Bower, "Review of engineering recommendation g5/4-1 stage 3 connections and higher order harmonics," *EA Technology*, pp. 1–69, 2013.

[120] W. Mingli, Q. Liu, S. Yang, H. Zhang, L. Wu, and J. Li, "A cascaded h-bridge based harmonic generator for traction network harmonic impedance measurement and measuring method," in *CHN Patent: CN105699779A*, Jun. 2016.

[121] L. Qiujiang, W. Mingli, Z. Junqi, S. Kejian, and W. Liran, "Resonant frequency identification based on harmonic injection measuring method for traction power supply systems," *IET Power Electron.*, vol. 11, no. 3, pp. 585–592, Mar. 2018.

[122] L. Qiujiang, W. Mingli, Z. Junqi, S. Kejian, and W. Liran, "Controllable harmonic generating method for harmonic impedance measurement of traction power supply systems based on phase shifted pwm," *Journal of Power Electronics*, vol. 18, no. 4, pp. 1140–1153, Jul. 2018.

Kejian Song was born in Hunan province, China. He received the B.Sc. degree in electrical engineering from Shaoyang University, Shaoyang, China, in 2010, the M.Sc. and Ph.D. degrees in electrical engineering from Beijing Jiaotong University (BJTU), Beijing, China in 2012 and 2017 respectively, where he is Postdoctoral Researcher. From December 2014 to December 2015, he was with the Australia Energy Research Institute, UNSW Australia, Sydney, as an exchanged Ph.D. student sponsored by China Scholarship Council. His research interests include modulation methods and control strategies for traction converters and electric power quality of traction power supply systems.

Wu Mingli was born in Hebei Province, China. He received his B.Sc. and M.Sc. degrees in Electrical Engineering from Southwest Jiaotong University, Chengdu, China, in 1993 and 1996, respectively, and his Ph.D. in Electrical Engineering from Beijing Jiaotong University, Beijing, China, in 2006. Since 2008, he has been a Professor at the School of Electrical Engineering, Beijing Jiaotong University. His research areas include power supply for electric railways, digital simulation of power systems, and electric power quality.

This article has been accepted for publication in a future issue of this journal, but has not been fully edited. Content may change prior to final publication. Citation information: DOI 10.1109/TPEL.2019.2928636, IEEE Transactions on Power Electronics

Shaobing Yang received his B.S. degree in electrical engineering from Shanghai Jiaotong University in 1995, and M.S. and Ph.D degrees in electrical engineering from Beijing Jiaotong University in 2009 and 2016, respectively. He is an associate professor of the School of Electrical Engineering in Beijing Jiaotong University. His current research areas include power system simulation, load modeling, demand side management, electric power quality, and load forecasting for electric vehicles.

Qiujiang Liu was born in Hebei province, China, on August 23, 1989. He received his B.Sc., M.Sc., and D.Sc degrees in Electrical Engineering from Beijing Jiaotong University (BJTU), Beijing, China, in 2012, 2014, and 2018 respectively. He is currently working in School of Electrical Engineering, BJTU. His research interests include power quality of electric railways and power electronics in power supply systems.

Vassilios G. Agelidis (S'89–M'91–SM'00–F'16) was born in Serres, Greece. He received the B.Eng. degree in electrical engineering from the Democritus University of Thrace, Thrace, Greece, in 1988, the M.S. degree in applied science from Concordia University, Montreal, QC, Canada, in 1992, and the Ph.D. degree in electrical engineering from Curtin University, Perth, Australia, in 1997. He has worked at Curtin University (1993–1999), University of Glasgow, U.K. (2000–2004), Murdoch University, Perth, Australia (2005–2006), the University of Sydney, Australia (2007–2010), and the University of New South Wales (UNSW), Sydney, Australia (2010-2016). He is currently a professor at the Department of Electrical Engineering, Technical University of Denmark. Dr. Agelidis received the Advanced Research Fellowship from the U.K.'s Engineering and Physical Sciences Research Council in 2004. He was the Vice-President Operations within the IEEE Power Electronics Society from 2006 to 2007. He was an AdCom Member of the IEEE Power Electronics Society from 2007 to 2009 and the Technical Chair of the 39th IEEE Power Electronics Specialists Conference, Rhodes, Greece, 2008.

Georgios Konstantinou (S'08–M'11) received the B.Eng. degree in electrical and computer engineering from the Aristotle University of Thessaloniki, Thessaloniki, Greece, in 2007 and the Ph.D. degree in electrical engineering from UNSW Sydney (The University of New South Wales), Australia, in 2012. From 2012 to 2015 he was a Research Associate at UNSW. He is currently a Senior Lecturer with the School of Electrical Engineering and Telecommunications at UNSW and an Australian Research Council (ARC) Early Career Research Fellow. His main research interests include multilevel converters, power electronics in HVDC, renewable energy and energy storage applications. He is an Associate Editor for IEEE Transactions on Power Electronics and IET Power Electronics.